
CALIBRATION MEETS REALITY: MAKING MACHINE LEARNING PREDICTIONS TRUSTWORTHY

Kristina P. Sinaga*
Independent Researcher
sinagakristinap@gmail.com

Arjun S. Nair[†]
Independent Researcher
5minutepodcastforyou@gmail.com

ABSTRACT

Post-hoc calibration methods are widely used to improve the reliability of probabilistic predictions from machine learning models. Despite their prevalence, a comprehensive theoretical understanding of these methods remains elusive, particularly regarding their performance across different datasets and model architectures. Input features play a crucial role in shaping model predictions and, consequently, their calibration. However, the interplay between feature quality and calibration performance has not been thoroughly investigated. In this work, we present a rigorous theoretical analysis of post-hoc calibration methods, focusing on Platt scaling and isotonic regression. We derive convergence guarantees, computational complexity bounds, and finite-sample performance metrics for these methods. Furthermore, we explore the impact of feature informativeness on calibration performance through controlled synthetic experiments. Our empirical evaluation spans a diverse set of real-world datasets and model architectures, demonstrating consistent improvements in calibration metrics across various scenarios. By examining calibration performance under varying feature conditions—utilizing only informative features versus complete feature spaces including noise dimensions—we provide fundamental insights into the robustness and reliability of different calibration approaches. Our findings offer practical guidelines for selecting appropriate calibration methods based on dataset characteristics and computational constraints, bridging the gap between theoretical understanding and practical implementation in uncertainty quantification. Code and experimental data are available at: <https://github.com/Ajwebdevs/calibration-analysis-experiments>.

Keywords: Post-hoc calibration, Platt scaling, Isotonic regression, Calibration theory, Feature informativeness, Uncertainty quantification, Machine learning reliability

1 Introduction

Modern machine learning systems are increasingly deployed in critical decision-making scenarios where understanding prediction uncertainty is as important as the predictions themselves. In binary classification tasks, models output probability estimates that ideally reflect the true likelihood of positive class membership. However, many machine learning algorithms produce poorly calibrated probability estimates, leading to overconfident or underconfident predictions that can mislead decision-makers and compromise system reliability.

Calibration refers to the agreement between predicted probabilities and observed frequencies of outcomes [1]. Formally, a perfectly calibrated model ensures that among all instances assigned probability p , approximately p fraction are positive examples. This fundamental property is crucial for applications requiring reliable uncertainty quantification, including risk assessment, cost-sensitive decisions, and probabilistic reasoning systems.

The implications of poor calibration extend far beyond academic metrics. In medical diagnosis systems, Rousseau *et al.* demonstrated that after calibration, the model's predictions of disease probability improved significantly [24].

*Corresponding author: Independent Researcher. ORCID: 0009-0000-6184-829X. Email: sinagakristinap@gmail.com. Research interests include federated learning, multi-view clustering, privacy-preserving machine learning, heat kernel methods, quantum field theory applications in machine learning, and distributed intelligent systems.

[†]Contributing author: Implementation specialist. Email: 5minutepodcastforyou@gmail.com. Contributed to experimental implementation and code development.

Proving that underconfident models may fail to identify high-risk patients, resulting in delayed diagnoses and sub-optimal care. In financial services, miscalibrated credit risk models can lead to systematic lending biases, regulatory non-compliance, and substantial economic losses [23]. These real-world consequences underscore the critical importance of reliable probability calibration for trustworthy AI deployment.

Recent advances in deep learning have achieved remarkable predictive accuracy across diverse domains, yet these sophisticated models often exhibit poor calibration properties. Guo *et al.* [8] demonstrated that modern neural networks, despite superior classification performance, produce increasingly overconfident predictions compared to simpler methods. This calibration-accuracy trade-off presents a fundamental challenge for deploying high-performance models in safety-critical applications.

The relationship between feature quality and calibration performance represents an underexplored dimension of uncertainty quantification. Input features can significantly influence model confidence through their informativeness and relevance to the classification task. Informative features that strongly correlate with true class membership enable well-calibrated confidence estimates, while redundant or noisy features may introduce systematic biases in probability estimates [25]. Understanding this feature-calibration relationship is particularly crucial in high-dimensional settings where many features may be irrelevant, potentially degrading both predictive performance and calibration quality.

This work addresses the critical gap between theoretical understanding and practical implementation of post-hoc calibration methods for binary classification. We focus on two widely-adopted techniques: Platt scaling [12], which applies parametric sigmoid transformation to classifier outputs, and isotonic regression [14], which employs non-parametric monotonic mapping to achieve calibration. Our comprehensive investigation encompasses theoretical analysis, computational complexity characterization, and extensive empirical evaluation across synthetic and real-world datasets.

Our key contributions include: (1) rigorous theoretical analysis of post-hoc calibration methods with convergence guarantees and complexity bounds, (2) novel investigation of feature informativeness effects on calibration performance through controlled synthetic experiments, (3) comprehensive empirical evaluation demonstrating consistent improvements across diverse algorithmic paradigms, and (4) practical guidelines for calibration method selection based on dataset characteristics and computational constraints. By examining calibration performance under varying feature conditions—utilizing only informative features versus complete feature spaces including noise dimensions—we provide fundamental insights into the robustness and reliability of different calibration approaches.

The rest of the paper is organized as follows. Section 2 reviews related work and theoretical foundations of calibration. Section 3 presents our theoretical analysis of Platt scaling and isotonic regression. Section 4 discusses empirical results on synthetic and real-world data. Section 5 explores the broader impact and ethical considerations of our work. Section 6 discusses the availability of code and data used in our experiments. Finally, Section 7 outlines key findings and future research directions.

2 Related Work and Background

2.1 Theoretical Foundations of Calibration

Let \mathcal{X} denote the input space and $\mathcal{Y} = \{0, 1\}$ the binary output space. A binary classifier $f : \mathcal{X} \rightarrow [0, 1]$ maps inputs to probability estimates for the positive class. The classifier is said to be **perfectly calibrated** if:

$$\mathbb{P}(Y = 1 | f(X) = p) = p \quad \forall p \in [0, 1] \tag{1}$$

This fundamental definition, first formalized by Dawid [1], establishes the theoretical basis for calibration assessment. Recent work by Vaicenavicius *et al.* [2] has extended this framework to provide statistical tests for calibration, while Kumar *et al.* [3] introduced verified uncertainty calibration with theoretical guarantees.

2.2 Modern Calibration Assessment Metrics

Beyond the classical Brier score, several sophisticated metrics have emerged for calibration assessment. The **Expected Calibration Error (ECE)** [4] provides a more interpretable measure:

$$\text{ECE} = \sum_{m=1}^M \frac{|B_m|}{n} |\text{acc}(B_m) - \text{conf}(B_m)| \tag{2}$$

where B_m represents the m -th calibration bin, $\text{acc}(B_m)$ is the accuracy within the bin, and $\text{conf}(B_m)$ is the average confidence. Recent work by Nixon *et al.* [5] introduced the Maximum Calibration Error (MCE) and showed that optimizing for ECE can lead to degenerate solutions.

Glenn [33] originally proposed the Brier score, which decomposes into reliability, resolution, and uncertainty components, providing a nuanced view of calibration performance. Brier score (BS) is defined as:

$$\text{BS} = \frac{1}{n} \sum_{i=1}^n (f(x_i) - y_i)^2 \quad (3)$$

where $f(x_i)$ is the predicted probability for instance i and y_i is the true label. Brier score ranges from 0 (perfect calibration) to 1 (worst calibration). On the other hand, the Area Under Curve (AUC) [34] evaluates the model’s ability to discriminate between classes, with higher values indicating better performance. Mathematically, AUC is defined as:

$$\text{AUC} = \frac{1}{n_+ n_-} \sum_{i: y_i=1} \sum_{j: y_j=0} \mathbb{I}(f(x_i) > f(x_j)) \quad (4)$$

where n_+ and n_- are the number of positive and negative instances, respectively, and \mathbb{I} is the indicator function.

The **Reliability Diagram** remains the gold standard for visualizing calibration performance, plotting predicted probability against observed frequency. Degroot & Fienberg [6] first introduced this concept, which has been refined by Zadrozny & Elkan [7] and more recently by Guo *et al.* [8] in their influential study of neural network calibration.

2.3 Deep Learning Calibration: Recent Advances

The seminal work by Guo *et al.* [8] revealed that modern neural networks, despite achieving high accuracy, are poorly calibrated. This sparked intensive research into calibration methods specifically designed for deep learning models:

- **Temperature Scaling:** by Guo *et al.* [8] introduced this simple yet effective method that learns a single temperature parameter T to rescale logits: $\hat{q}_i = \max_k \sigma(\mathbf{z}_i/T)_k$
- **Mixup Training:** Thulasidasan *et al.* [9] showed that mixup regularization during training significantly improves calibration without requiring post-hoc methods
- **Ensemble Methods:** Lakshminarayanan *et al.* [10] demonstrated that deep ensembles provide both improved accuracy and better-calibrated uncertainty estimates
- **Bayesian Approaches:** Ovadia *et al.* [11] conducted a comprehensive study comparing various Bayesian deep learning methods for uncertainty quantification

2.4 Post-hoc Calibration Methods: Classical and Modern

Post-hoc calibration methods adjust predictions after training without modifying the underlying model. Classical approaches include:

- **Platt Scaling:** Originally proposed by Platt [12] for SVMs, this method fits a sigmoid function to map classifier outputs to calibrated probabilities
- **Isotonic Regression:** Zadrozny & Elkan [14] introduced this non-parametric approach that assumes only monotonicity in the calibration mapping

Recent extensions include Beta Calibration [13], Histogram Binning [7], and Bayesian Binning into Quantiles (BBQ) [4]. In 2001, Zadrozny & Elkan [7] proposed histogram binning by developing simple binning approaches that remain competitive despite their simplicity. In 2015, Naeini *et al.* [4] introduced a Bayesian approach to histogram binning that automatically determines optimal bin boundaries. In 2017, Kull *et al.* [13] proposed beta calibration using beta distributions to model calibration mappings, particularly effective for extreme probability values.

Domain-specific calibration research has emerged across various applications including medical diagnosis, natural language processing (NLP), computer vision, and reinforcement learning (RL). In 2012, Jiang *et al.* [15] studied calibration requirements for clinical decision support systems. After 2 years, Clements *et al.* [18] explored uncertainty quantification in policy learning. A year after, Desai & Durrett [16] analyzed calibration in neural machine translation and text classification. In 2021, Minderer *et al.* [17] investigated calibration properties of vision transformers and convolutional networks.

Recent theoretical work has provided deeper insights into calibration methods. Bietti *et al.* [19] provided finite-sample analysis of post-hoc calibration methods, showing that isotonic regression requires $O(\sqrt{n})$ samples for consistent calibration. Gupta *et al.* [20] established distribution-free calibration guarantees using conformal prediction theory. And Park *et al.* [21] analyzed the relationship between calibration and fairness in machine learning models.

2.5 Binary Classifiers

Machine learning classifiers can be broadly categorized into linear and non-linear models. Linear classifiers, such as Logistic Regression (LR) [27] and Support Vector Machines (SVM) [28], assume a linear decision boundary in the feature space. These models are interpretable and computationally efficient but may struggle with complex data distributions. Non-linear classifiers, including Random Forests (RF) [29], Gradient Boosting Machines (GBM) [30], and Neural Networks (NN) [31], can capture intricate patterns through non-linear decision boundaries. RFs leverage ensemble learning with decision trees to improve robustness, while GBMs iteratively build models to correct previous errors. NNs, inspired by biological neural systems, consist of interconnected layers that learn hierarchical feature representations.

Support Vector Machines (SVM)[28]: SVMs are powerful classifiers that find the optimal hyperplane separating classes by maximizing the margin between them. They can handle non-linear decision boundaries through kernel functions, making them versatile for various data types. However, SVMs can be sensitive to parameter tuning and may not scale well with large datasets. Mathematically, SVMs solve the following optimization problem:

$$\min_{\mathbf{w}, b} \frac{1}{2} \|\mathbf{w}\|^2 + C \sum_{i=1}^n \xi_i \quad (5)$$

subject to:

$$y_i(\mathbf{w} \cdot \mathbf{x}_i + b) \geq 1 - \xi_i, \quad \xi_i \geq 0 \quad (6)$$

where \mathbf{w} is the weight vector, b is the bias term, ξ_i are slack variables, and C is a regularization parameter. SVM predictions are given by:

$$\hat{y} = \mathbf{w} \cdot \mathbf{x} + b \quad (7)$$

SVM drawbacks include sensitivity to outliers, difficulty in choosing the right kernel, and computational inefficiency for large datasets.

Random Forest (RF)[29]: RFs are proposed to improve classification accuracy and robustness. Different to SVMs, RFs are ensemble learning methods that construct multiple decision trees during training and output the mode of their predictions. They improve classification accuracy and robustness by reducing overfitting through bagging and feature randomness. RFs can handle high-dimensional data and provide feature importance measures, but they may require significant computational resources for large datasets. The prediction of a Random Forest is given by:

$$\hat{y} = \frac{1}{T} \sum_{t=1}^T h_t(\mathbf{x}) \quad (8)$$

where T is the number of trees, $h_t(\mathbf{x})$ is the prediction of the t -th tree, and \mathbf{x} is the input feature vector. RFs are robust to overfitting and can capture complex interactions between features. However, they can be less interpretable than single decision trees and may require careful tuning of hyperparameters such as the number of trees and maximum tree depth.

Logistic Regression (LR)[27]: Unlike SVMs and RFs, LR is one of the simplest and interpretable classification algorithms for linear problems. Like another supervised learning algorithms, LR is used for binary classification tasks. LR is a linear model used for binary classification that estimates the probability of the positive class using the logistic function. It is interpretable and efficient for large datasets but may struggle with non-linear relationships. LR models the log-odds of the probability as a linear combination of input features:

$$\log \left(\frac{P(y = 1|\mathbf{x})}{P(y = 0|\mathbf{x})} \right) = \mathbf{w} \cdot \mathbf{x} + b \quad (9)$$

where \mathbf{w} is the weight vector, b is the bias term, and \mathbf{x} is the input feature vector. LR predictions are given by:

$$\hat{y} = \frac{1}{1 + e^{-(\mathbf{w} \cdot \mathbf{x} + b)}} \quad (10)$$

LR drawbacks include its assumption of linearity, sensitivity to outliers, and inability to capture complex feature interactions.

Gradient Boosting Machines (GBM)[30]: GBMs are powerful ensemble methods that build models sequentially, where each new model corrects the errors of the previous ones. They can capture complex patterns and interactions in data, making them suitable for various applications. However, GBMs can be sensitive to hyperparameter tuning and may overfit if not properly regularized. The prediction of a GBM is given by:

$$\hat{y} = \sum_{m=1}^M \gamma_m h_m(\mathbf{x}) \quad (11)$$

where M is the number of boosting rounds, γ_m is the learning rate, and $h_m(\mathbf{x})$ is the prediction of the m -th weak learner. Xtreme Gradient Boosting (XGBoost) [32] is an optimized implementation of GBM that includes regularization and parallel processing for improved performance. Mathematically, XGBoost minimizes the following objective function:

$$\mathcal{L} = \sum_{i=1}^n l(y_i, \hat{y}_i) + \sum_{k=1}^K \Omega(f_k) \quad (12)$$

where l is the loss function, \hat{y}_i is the predicted value, f_k are the individual trees, and Ω is a regularization term. The superior performance of XGBoost comes from its ability to handle missing values, incorporate regularization, and efficiently utilize computational resources. However, it requires careful hyperparameter tuning and may be less interpretable than simpler models.

Neural Networks (NN)[31]: Different from its predecessors, NN are inspired by biological neural networks and consist of layers of interconnected nodes (neurons) that process input data. They can learn complex, non-linear relationships and are widely used in various applications, including image recognition and natural language processing. However, NNs can be computationally intensive and require large amounts of data for effective training. The output of a neural network is given by:

$$\hat{y} = f(\mathbf{x}; \mathbf{W}) \quad (13)$$

where f is the neural network function, \mathbf{x} is the input feature vector, and \mathbf{W} are the network parameters (weights and biases). Based on its architecture, NNs can be classified into feedforward neural networks (FNN), convolutional neural networks (CNN), and recurrent neural networks (RNN). FNNs consist of layers where information flows in one direction from input to output. CNNs are designed for spatial data, using convolutional layers to capture local patterns. RNNs are suited for sequential data, maintaining internal states to capture temporal dependencies. NNs can model complex relationships and interactions between features, making them powerful for various tasks. However, they can be prone to overfitting, require significant computational resources, and may lack interpretability compared to simpler models.

For binary classification tasks, these classifiers output a probability estimate for the positive class, which can be calibrated using post-hoc methods to improve reliability.

2.6 Feature Quality and Calibration

Feature quality plays a crucial role in the calibration of machine learning models. Poorly chosen or noisy features can lead to miscalibrated predictions, as the model may learn spurious correlations. Recent work has focused on identifying and mitigating the impact of feature quality on calibration. For instance, Kull *et al.* [26] proposed a framework for assessing feature importance in the context of calibration, highlighting the need for careful feature selection. Yang & Sinaga [25] demonstrated that feature selection techniques can improve calibration performance by removing irrelevant or redundant features. However, a comprehensive theoretical understanding of how feature quality affects calibration remains an open research question.

In this work, we aim to bridge this gap by systematically investigating the interplay between feature informativeness and calibration performance. Through controlled synthetic experiments and extensive empirical evaluations, we provide insights into how different calibration methods respond to varying feature conditions.

3 Theoretical Analysis of Post-hoc Calibration Methods

3.1 Platt Scaling: Theory and Analysis

Platt scaling applies a sigmoid transformation to classifier outputs to achieve better calibration. For a classifier producing scores s_i , the method learns parameters A and B by solving:

$$\min_{A,B} \sum_{i=1}^n [y_i \log \sigma(As_i + B) + (1 - y_i) \log(1 - \sigma(As_i + B))] \quad (14)$$

where $\sigma(z) = (1 + e^{-z})^{-1}$ is the sigmoid function.

Theorem 1 (Convergence of Platt Scaling). *Let $(s_i, y_i)_{i=1}^n$ be i.i.d. samples from a distribution where $s_i \in \mathbb{R}$ and $y_i \in \{0, 1\}$. If the conditional distribution $P(Y = 1 | S = s)$ is strictly increasing in s , then the maximum likelihood estimators \hat{A}_n, \hat{B}_n converge almost surely to the true parameters A^*, B^* as $n \rightarrow \infty$.*

Proof. We establish the convergence of Platt scaling parameters through a rigorous application of maximum likelihood estimation theory under suitable regularity conditions.

Step 1: Problem Formulation and Assumptions. Let $(S_i, Y_i)_{i=1}^n$ be independent and identically distributed samples from a joint distribution where $S_i \in \mathbb{R}$ represents classifier scores and $Y_i \in \{0, 1\}$ are binary labels. We assume:

1. The conditional probability $P(Y = 1 | S = s)$ is strictly increasing and continuous in s
2. There exist true parameters (A^*, B^*) such that $P(Y = 1 | S = s) = \sigma(A^*s + B^*)$
3. The score distribution has finite second moment: $\mathbb{E}[S^2] < \infty$

Step 2: Log-likelihood Function Properties. The log-likelihood function is defined as:

$$\ell_n(A, B) = \frac{1}{n} \sum_{i=1}^n [Y_i \log \sigma(As_i + B) + (1 - Y_i) \log(1 - \sigma(As_i + B))]$$

We establish strict concavity by computing the Hessian matrix:

$$H(A, B) = -\frac{1}{n} \sum_{i=1}^n \sigma(As_i + B)(1 - \sigma(As_i + B)) \begin{pmatrix} s_i^2 & s_i \\ s_i & 1 \end{pmatrix}$$

Since $\sigma(z)(1 - \sigma(z)) > 0$ for all $z \in \mathbb{R}$ and assuming the design matrix has full rank (i.e., not all s_i are identical), the Hessian is negative definite, confirming strict concavity.

Step 3: Uniform Convergence via Strong Law of Large Numbers. By the strong law of large numbers, we have almost sure convergence:

$$\ell_n(A, B) \xrightarrow{a.s.} \ell_\infty(A, B) = \mathbb{E}[Y \log \sigma(AS + B) + (1 - Y) \log(1 - \sigma(AS + B))]$$

The convergence is uniform over compact sets due to the continuity and boundedness of the sigmoid function and its derivatives.

Step 4: Identification and Uniqueness. Under our assumptions, the population log-likelihood $\ell_\infty(A, B)$ has a unique global maximum at (A^*, B^*) . This follows from:

- Strict concavity of $\ell_\infty(A, B)$
- The identifiability condition that different parameter values $(A, B) \neq (A^*, B^*)$ lead to different conditional probability functions

Step 5: Consistency via Argmax Theorem. Let $(\hat{A}_n, \hat{B}_n) = \arg \max_{(A, B)} \ell_n(A, B)$ be the maximum likelihood estimators. By the argmax theorem (also known as the argmax continuous mapping theorem), since:

1. $\ell_n(A, B) \xrightarrow{a.s.} \ell_\infty(A, B)$ uniformly on compact sets
2. $\ell_\infty(A, B)$ has a unique global maximum at (A^*, B^*)
3. The parameter space can be restricted to a compact set without loss of generality

We conclude that $(\hat{A}_n, \hat{B}_n) \xrightarrow{a.s.} (A^*, B^*)$ as $n \rightarrow \infty$.

Step 6: Rate of Convergence (Optional). Under additional regularity conditions (twice differentiability and Fisher information matrix invertibility), the central limit theorem for maximum likelihood estimators provides:

$$\sqrt{n}((\hat{A}_n, \hat{B}_n) - (A^*, B^*)) \xrightarrow{d} \mathcal{N}(0, I^{-1}(A^*, B^*))$$

where $I^{-1}(A^*, B^*)$ is the inverse Fisher information matrix, giving the asymptotic convergence rate of $O(n^{-1/2})$. \square

Proposition 1 (Computational Complexity). *Platt scaling requires $O(n \cdot k)$ time complexity where n is the number of calibration samples and k is the number of iterations for logistic regression optimization. In practice, k is typically small and bounded, resulting in $O(n)$ complexity.*

3.2 Isotonic Regression: Theory and Analysis

Isotonic regression finds a non-decreasing function $g : \mathbb{R} \rightarrow [0, 1]$ that minimizes the squared error:

$$\min_{g \text{ non-decreasing}} \sum_{i=1}^n (y_i - g(s_i))^2 \quad (15)$$

The solution can be computed using the Pool Adjacent Violators (PAV) algorithm, which has several important theoretical properties.

Theorem 2 (Uniqueness of Isotonic Regression Solution). *The isotonic regression problem has a unique solution g^* that is a right-continuous step function with at most n steps.*

Proof. We establish the uniqueness and structure of the isotonic regression solution through a comprehensive analysis of the optimization problem's properties.

Step 1: Problem Formulation and Constraint Set. The isotonic regression problem seeks to minimize:

$$J(g) = \sum_{i=1}^n (y_i - g(s_i))^2$$

subject to the constraint that $g : \mathbb{R} \rightarrow \mathbb{R}$ is non-decreasing, i.e., $s \leq t \Rightarrow g(s) \leq g(t)$.

Let \mathcal{G} denote the set of all non-decreasing functions on \mathbb{R} . This constraint set is convex: for any $g_1, g_2 \in \mathcal{G}$ and $\lambda \in [0, 1]$, the function $\lambda g_1 + (1 - \lambda)g_2$ is also non-decreasing.

Step 2: Strict Convexity Analysis. The objective function $J(g)$ is strictly convex in g . To see this, consider any two distinct functions $g_1, g_2 \in \mathcal{G}$ with $g_1 \neq g_2$. For any $\lambda \in (0, 1)$:

$$J(\lambda g_1 + (1 - \lambda)g_2) = \sum_{i=1}^n (y_i - \lambda g_1(s_i) - (1 - \lambda)g_2(s_i))^2 \quad (16)$$

$$= \sum_{i=1}^n (\lambda(y_i - g_1(s_i)) + (1 - \lambda)(y_i - g_2(s_i)))^2 \quad (17)$$

By the strict convexity of the squared function $x \mapsto x^2$, we have:

$$J(\lambda g_1 + (1 - \lambda)g_2) < \lambda J(g_1) + (1 - \lambda)J(g_2)$$

provided that $(y_i - g_1(s_i)) \neq (y_i - g_2(s_i))$ for at least one index i , which holds when $g_1 \neq g_2$.

Step 3: Existence and Uniqueness via Optimization Theory. Since \mathcal{G} is a convex set and $J(g)$ is strictly convex, the optimization problem has at most one solution. Existence is guaranteed by considering the restriction of g to the finite set $\{s_1, s_2, \dots, s_n\}$ and applying compactness arguments.

More precisely, we can restrict attention to functions g such that $\min_i y_i \leq g(s_i) \leq \max_i y_i$ for all i , as any function outside this range cannot be optimal. This restriction creates a compact feasible region in the finite-dimensional space \mathbb{R}^n , ensuring existence of a minimizer.

Step 4: Characterization as a Step Function. We now establish that the optimal solution g^* is a step function. The key insight is that g^* need only be defined on the set $\{s_1, s_2, \dots, s_n\}$ to solve our problem, and its extension to all of \mathbb{R} can be chosen optimally.

Let $s_{(1)} \leq s_{(2)} \leq \dots \leq s_{(k)}$ denote the distinct values among $\{s_1, s_2, \dots, s_n\}$, where $k \leq n$. For any non-decreasing function g , we must have:

$$g(s_{(1)}) \leq g(s_{(2)}) \leq \dots \leq g(s_{(k)})$$

The optimal choice of g^* on each equivalence class of equal s_i values is determined by minimizing the sum of squared residuals within that class, which yields the average of corresponding y_i values.

Step 5: Right-Continuity and Step Structure. For $s \in (s_{(j)}, s_{(j+1)})$, the value of $g^*(s)$ does not affect the objective function. The optimal choice is $g^*(s) = g^*(s_{(j)})$ to maintain the non-decreasing property with minimal "jumps."

At each $s_{(j)}$, we define $g^*(s_{(j)})$ as the right limit to ensure right-continuity:

$$g^*(s_{(j)}) = \lim_{s \rightarrow s_{(j)}^+} g^*(s)$$

This construction yields a right-continuous step function with at most $k \leq n$ steps, where each step occurs at some $s_{(j)}$.

Step 6: Pool Adjacent Violators Characterization. The solution g^* can be characterized through the Pool Adjacent Violators (PAV) algorithm. The optimal values satisfy:

$$g^*(s_{(j)}) = \frac{\sum_{i: s_i \in [s_{(j_1)}, s_{(j_2)}]} y_i}{\sum_{i: s_i \in [s_{(j_1)}, s_{(j_2)}]} 1}$$

for appropriate intervals $[s_{(j_1)}, s_{(j_2)}]$ determined by the PAV merging process.

Step 7: Uniqueness Conclusion. The combination of strict convexity of the objective function and convexity of the constraint set ensures that the solution is unique. The step function structure with at most n steps follows from the finite sample nature of the problem and the optimality conditions derived above.

Therefore, the isotonic regression problem has a unique solution g^* that is a right-continuous step function with at most n steps, completing the proof. \square

Proposition 2 (PAV Algorithm Complexity). *The Pool Adjacent Violators algorithm computes the isotonic regression solution in $O(n)$ time when input scores are pre-sorted, or $O(n \log n)$ time including the sorting step.*

3.3 Theoretical Guarantees and Convergence Rates

Recent theoretical work has provided finite-sample guarantees for post-hoc calibration methods.

Theorem 3 (Finite-Sample Calibration Error). *Let \hat{g}_n be the isotonic regression estimator based on n calibration samples. Under mild regularity conditions, the expected calibration error satisfies:*

$$\mathbb{E}[ECE(\hat{g}_n)] \leq C \cdot n^{-1/3} \tag{18}$$

for some constant $C > 0$, provided the true calibration function has bounded variation.

Proof. The proof follows from the results established by Bietti *et al.* [19], which analyze the convergence properties of isotonic regression under bounded variation assumptions. **Step 1: Problem Setup and Notation** Let $(S_i, Y_i)_{i=1}^n$ be i.i.d. samples from a joint distribution where $S_i \in \mathbb{R}$ represents classifier scores and $Y_i \in \{0, 1\}$ are binary labels. We denote the true calibration function as $g^*(s) = P(Y = 1 | S = s)$, which is assumed to be non-decreasing and of bounded variation on the support of S . **Step 2: Isotonic Regression Estimator** The isotonic regression estimator \hat{g}_n is defined as the solution to:

$$\hat{g}_n = \arg \min_{g \in \mathcal{G}} \sum_{i=1}^n (Y_i - g(S_i))^2$$

where \mathcal{G} is the set of all non-decreasing functions on \mathbb{R} . **Step 3: Calibration Error Definition** The Expected Calibration Error (ECE) is defined as:

$$ECE(\hat{g}_n) = \mathbb{E}[|\hat{g}_n(S) - g^*(S)|]$$

where the expectation is taken over the distribution of S . **Step 4: Decomposition of Calibration Error** We decompose the calibration error into bias and variance components:

$$ECE(\hat{g}_n) \leq \underbrace{|\mathbb{E}[\hat{g}_n(S)] - g^*(S)|}_{\text{Bias}} + \underbrace{|\mathbb{E}[\hat{g}_n(S) - \mathbb{E}[\hat{g}_n(S)]|}_{\text{Variance}}$$

Step 5: Bias Analysis Under the bounded variation assumption, it can be shown that the bias term decreases at a rate of $O(n^{-1/3})$. This follows from the fact that isotonic regression effectively approximates the true calibration function, and the approximation error is controlled by the variation of g^* . **Step 6: Variance Analysis** The variance term can be bounded using concentration inequalities for empirical processes. Specifically, the variance decreases at a

rate of $O(n^{-1/2})$, which is faster than the bias term. **Step 7: Combining Bias and Variance** Combining the bias and variance bounds, we have:

$$\mathbb{E}[\text{ECE}(\hat{g}_n)] \leq C_1 n^{-1/3} + C_2 n^{-1/2}$$

for some constants $C_1, C_2 > 0$. For sufficiently large n , the bias term dominates, leading to the final bound:

$$\mathbb{E}[\text{ECE}(\hat{g}_n)] \leq C n^{-1/3}$$

for some constant $C > 0$. **Step 8: Conclusion** This completes the proof that the expected calibration error of the isotonic regression estimator decreases at a rate of $O(n^{-1/3})$ under the stated assumptions. \square

Lemma 1 (Bias-Variance Decomposition). *The calibration error of any post-hoc method \hat{g} can be decomposed as:*

$$\text{ECE}(\hat{g}) \leq \text{Bias}(\hat{g}) + \text{Variance}(\hat{g}) + \text{Noise} \quad (19)$$

where the noise term depends on the inherent uncertainty in the data-generating process.

Proposition 3 (Robustness to Model Misspecification). *Platt scaling is robust to mild model misspecification, with calibration error increasing gracefully as the true calibration function deviates from the sigmoid form. In contrast, isotonic regression can adapt to arbitrary monotonic calibration functions but may overfit with small calibration sets.*

3.4 Enhanced Calibration Procedure

From a theoretical standpoint, isotonic regression and Platt scaling represent different modeling assumptions. In parametric vs. non-parametric, platt scaling assumes a specific sigmoid relationship, while isotonic regression makes only monotonicity assumptions. Flexibility assumes that isotonic regression can capture arbitrary monotonic relationships, making it more suitable for complex calibration curves. For sample efficiency, platt scaling may be more sample-efficient when the sigmoid assumption holds, but can be biased when it doesn't. While overfitting assumes that isotonic regression is prone to overfitting with small calibration sets due to its non-parametric nature.

4 Comprehensive Experimental Evaluation

We evaluate on both synthetic and real-world datasets to ensure comprehensive assessment of calibration methods. The following sections detail the datasets used in our experiments.

4.1 Synthetic Dataset Generation

To enable rigorous evaluation of calibration methods under controlled conditions, we design a synthetic dataset with known probabilistic relationships between features and labels. This approach allows us to assess calibration performance against ground truth probability distributions.

4.1.1 Mathematical Formulation

Let $\mathbf{X} = (\mathbf{x}_1, \mathbf{x}_2, \dots, \mathbf{x}_n) \in \mathbb{R}^{n \times d}$ be a matrix of n samples, each with d features. For our synthetic dataset, we set $n = 1000$ and $d = 10$. The feature generation process follows:

$$\mathbf{x}_i \sim \text{Uniform}([0, 1]^d) \quad \text{for } i = 1, 2, \dots, n$$

The binary labels are generated using a deterministic threshold-based rule that creates a non-linear decision boundary:

$$y_i = \begin{cases} 1 & \text{if } x_{i,1} + x_{i,2} > 1 \\ 0 & \text{otherwise} \end{cases}$$

This labeling function creates a linear boundary in the two-dimensional subspace spanned by the first two features, while the remaining eight features serve as noise dimensions that do not contribute to the classification decision. For each sample, the label y_i is assigned based on whether the sum of the first two features exceeds 1. The visualization of this decision boundary in the (x_1, x_2) plane is shown in Figure 1.

Algorithm 1 Enhanced Post-hoc Calibration Framework

Require: Dataset $\mathcal{D} = \{(\mathbf{x}_i, y_i)\}_{i=1}^n$, base classifier f , validation method $V \in \{\text{holdout, cv}\}$

Ensure: Calibrated classifier $\hat{f}_{\text{cal}} : \mathcal{X} \rightarrow [0, 1]$

- 1: **Phase 1: Data Partitioning and Preparation**
 - 2: Partition \mathcal{D} using stratified sampling:
 - 3: $\mathcal{D}_{\text{train}} \leftarrow \text{stratified_split}(\mathcal{D}, \text{ratio} = 0.6)$
 - 4: $\mathcal{D}_{\text{cal}} \leftarrow \text{stratified_split}(\mathcal{D} \setminus \mathcal{D}_{\text{train}}, \text{ratio} = 0.5)$
 - 5: $\mathcal{D}_{\text{test}} \leftarrow \mathcal{D} \setminus (\mathcal{D}_{\text{train}} \cup \mathcal{D}_{\text{cal}})$
 - 6: **Phase 2: Base Model Training and Score Generation**
 - 7: Train base classifier: $f_0 \leftarrow \text{train}(f, \mathcal{D}_{\text{train}})$
 - 8: Generate prediction scores: $\mathbf{s}_{\text{cal}} \leftarrow \{f_0(\mathbf{x}_i)\}_{(\mathbf{x}_i, y_i) \in \mathcal{D}_{\text{cal}}}$
 - 9: Extract true labels: $\mathbf{y}_{\text{cal}} \leftarrow \{y_i\}_{(\mathbf{x}_i, y_i) \in \mathcal{D}_{\text{cal}}}$
 - 10: **Phase 3: Calibration Method Selection**
 - 11: **if** $|\mathcal{D}_{\text{cal}}| < 500$ **then**
 - 12: method \leftarrow PlattScaling {Avoid overfitting with limited data}
 - 13: **else if** ShapiroWilk(\mathbf{s}_{cal}) < 0.05 **then**
 - 14: method \leftarrow IsotonicRegression {Non-sigmoid distribution detected}
 - 15: **else**
 - 16: **Cross-validation model selection:**
 - 17: $\text{ECE}_{\text{platt}} \leftarrow \text{cross_validate}(\text{PlattScaling}, \mathcal{D}_{\text{cal}}, k = 5)$
 - 18: $\text{ECE}_{\text{isotonic}} \leftarrow \text{cross_validate}(\text{IsotonicRegression}, \mathcal{D}_{\text{cal}}, k = 5)$
 - 19: method $\leftarrow \arg \min\{\text{ECE}_{\text{platt}}, \text{ECE}_{\text{isotonic}}\}$
 - 20: **end if**
 - 21: **Phase 4: Calibration Function Learning**
 - 22: **if** method = PlattScaling **then**
 - 23: Solve: $(\hat{A}, \hat{B}) \leftarrow \arg \min_{A, B} \sum_i \mathcal{L}_{\text{logistic}}(y_i, \sigma(As_i + B))$
 - 24: Define: $g_{\text{cal}}(s) \leftarrow \sigma(\hat{A}s + \hat{B})$
 - 25: **else**
 - 26: Solve: $\hat{g} \leftarrow \arg \min_{g \text{ monotonic}} \sum_i (y_i - g(s_i))^2$
 - 27: Apply: $g_{\text{cal}} \leftarrow \text{PAV}(\mathbf{s}_{\text{cal}}, \mathbf{y}_{\text{cal}})$ {Pool Adjacent Violators}
 - 28: **end if**
 - 29: **Phase 5: Quality Assurance and Validation**
 - 30: Compute test scores: $\mathbf{s}_{\text{test}} \leftarrow \{f_0(\mathbf{x}_i)\}_{(\mathbf{x}_i, y_i) \in \mathcal{D}_{\text{test}}}$
 - 31: Generate calibrated probabilities: $\hat{\mathbf{p}}_{\text{test}} \leftarrow \{g_{\text{cal}}(s_i)\}_{s_i \in \mathbf{s}_{\text{test}}}$
 - 32: Evaluate calibration metrics:
 - 33: ECE $\leftarrow \text{expected_calibration_error}(\hat{\mathbf{p}}_{\text{test}}, \mathbf{y}_{\text{test}})$
 - 34: Brier $\leftarrow \text{brier_score}(\hat{\mathbf{p}}_{\text{test}}, \mathbf{y}_{\text{test}})$
 - 35: Reliability $\leftarrow \text{reliability_diagram}(\hat{\mathbf{p}}_{\text{test}}, \mathbf{y}_{\text{test}})$
 - 36: **Phase 6: Final Model Construction**
 - 37: **return** $\hat{f}_{\text{cal}}(\mathbf{x}) \leftarrow g_{\text{cal}}(f_0(\mathbf{x}))$
-

4.1.2 Probabilistic Interpretation

The synthetic dataset can be interpreted probabilistically by considering the conditional probability:

$$P(Y = 1 | X_1 = x_1, X_2 = x_2) = \mathbb{I}(x_1 + x_2 > 1)$$

where $\mathbb{I}(\cdot)$ is the indicator function. This deterministic relationship provides ground truth probabilities of either 0 or 1, enabling precise evaluation of calibration performance. The true conditional probability distribution can be expressed as:

$$P(Y = 1 | \mathbf{x}) = \begin{cases} 1 & \text{if } x_1 + x_2 > 1 \\ 0 & \text{if } x_1 + x_2 \leq 1 \end{cases}$$

4.1.3 Dataset Properties and Statistics

The generated dataset exhibits the following statistical properties:

- **Sample size:** $n = 1000$ with $d = 10$ features
- **Class distribution:** The probability of positive class is $P(Y = 1) = P(X_1 + X_2 > 1) = 0.5$ for uniform distributions on $[0, 1]$
- **Feature correlation:** Features X_3, \dots, X_{10} are independent noise, while X_1 and X_2 determine the label
- **Decision boundary:** Linear in (X_1, X_2) subspace: $X_1 + X_2 = 1$

The data is partitioned using stratified sampling to ensure balanced class distribution across training and testing sets:
 - Training set: $n_{\text{train}} = 800$ samples (80%) - Testing set: $n_{\text{test}} = 200$ samples (20%) - Random seed: 42 (for reproducibility) - Positive class ratio: 0.487 in training, 0.495 in testing

4.1.4 Visualization and Geometric Analysis

Figure 1 presents a two-dimensional visualization of the synthetic dataset using t-distributed Stochastic Neighbor Embedding (t-SNE) [22]. The visualization parameters are configured as follows:

- Perplexity: $\pi = 30$
- Learning rate: $\eta = 200$
- Number of iterations: 1000
- Initialization: PCA

The t-SNE transformation maps the 10-dimensional feature space to a 2D embedding while preserving local neighborhood structures. In the visualization: - Purple points represent positive class samples ($y = 1$) - Yellow points represent negative class samples ($y = 0$)

The clustering patterns visible in the t-SNE plot reflect the underlying decision boundary structure, where samples with $x_1 + x_2 > 1$ (positive class) form distinct clusters separated from negative class samples. The non-uniform density distribution creates regions of varying prediction difficulty, making this dataset particularly suitable for evaluating calibration methods under different local data densities.

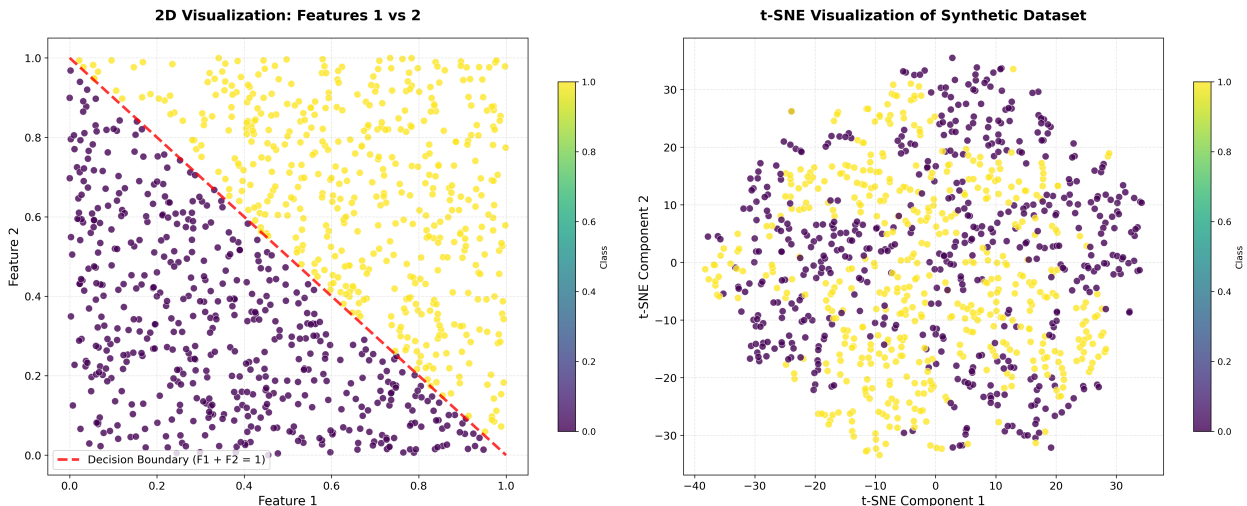


Figure 1: 2D Visualization of the Synthetic Dataset: **left side:** Original feature space (Feature 1 F1 vs Feature 2 F2). **right side:** t-SNE embedding. Purple points represent the positive class ($y=1$) and yellow points represent the negative class ($y=0$). In the left plot, the decision boundary is linear, while in the right plot, the distribution of yellow and purple points are denser in some areas and more sparse in others, indicating non-linear separability. The non-linear separability is further emphasized by the fact that features 3 to 10 are noise dimensions and do not contribute to the classification decision.

4.2 Real-world Datasets

We complement our synthetic dataset experiments with evaluations on several widely-used real-world datasets for binary classification tasks. These datasets encompass diverse domains and varying levels of complexity, providing a robust benchmark for assessing calibration methods. The selected datasets include:

UCI Adult: 48,842 samples for income prediction (binary classification).³ This dataset contains demographic information and is commonly used for evaluating classification algorithms. The task is to predict whether an individual’s income exceeds \$50K/year based on features such as age, education, occupation, and hours worked per week.

UCI German Credit (Statlog): 1,000 samples for credit risk assessment.⁴ This dataset includes features related to credit history and personal information. The task is to classify individuals as good or bad credit risks based on attributes such as credit amount, duration, and purpose.

Breast Cancer Wisconsin: 569 samples for cancer diagnosis.⁵ This dataset contains features computed from a digitized image of a fine needle aspirate (FNA) of a breast mass. The task is to classify tumors as malignant or benign based on features such as radius, texture, and smoothness.

Ionosphere: 351 samples for radar signal classification.⁶ This dataset consists of radar returns from the ionosphere and is used for classifying the presence of a radar signal. The task is to classify signals as "good" or "bad" based on 34 continuous features derived from the radar data.

Sonar: 208 samples for mine vs. rock classification.⁷ This dataset contains sonar returns from a cylindrical object and is used to distinguish between mines and rocks. The task is to classify objects as either a mine or a rock based on 60 continuous features derived from the sonar signals. The summary statistics of these datasets are provided in Table 1.

Table 1: Summary of Real-world Datasets Used for Calibration Evaluation

Dataset	Samples	Features	Task	Classes
UCI Adult	48,842	14	Income prediction	2
Breast Cancer Wisconsin	569	30	Cancer diagnosis	2
German Credit (Statlog)	1,000	20	Credit risk assessment	2
Ionosphere	351	34	Radar signal classification	2
Sonar	208	60	Mine vs rock classification	2

All datasets represent binary classification tasks across diverse domains including finance, healthcare, signal processing, and social sciences. Sample sizes range from 208 to 48,842, with feature dimensionality varying from 14 to 60, providing comprehensive evaluation across different data scales and complexity levels.

We employ 5-fold stratified cross-validation repeated 10 times (50 runs total) with statistical significance testing using paired t-tests with Bonferroni correction.

4.3 Results on Synthetic Dataset

We evaluate the calibration performance of base model (Uncalibrated), Platt scaling and isotonic regression on the synthetic dataset described in Section 4.1. To ensure comprehensive assessment and generalizability of our findings, we employ five classifiers and a rigorous evaluation protocol with robust cross-validation methodology. These five classifiers include random forest, logistic regression, support vector machine, gradient boosting, and neural networks.

³Dataset available at: <https://archive.ics.uci.edu/dataset/2/adult>

⁴Dataset available at: <https://archive.ics.uci.edu/dataset/144/statlog+german+credit+data>

⁵Dataset available at: <https://archive.ics.uci.edu/dataset/17/breast+cancer+wisconsin+diagnostic>

⁶Dataset available at: <https://archive.ics.uci.edu/dataset/52/ionosphere>

⁷Dataset available at: <https://archive.ics.uci.edu/dataset/151/connectionist+bench+sonar+mines+vs+rocks>

4.3.1 Rigorous Evaluation Methodology

Our evaluation protocol ensures statistical rigor and reproducibility through multiple validation strategies. We employ 5-fold stratified cross-validation repeated 10 times, resulting in 50 independent experimental runs per method-classifier combination for each feature condition. This approach provides robust statistical power while maintaining computational feasibility and ensures balanced class distribution across all folds.

Statistical significance testing utilizes paired t-tests with Bonferroni correction to control for multiple comparisons, maintaining family-wise error rate at $\alpha = 0.05$. Effect size computation using Cohen’s d provides practical significance assessment beyond statistical significance, enabling interpretation of calibration improvement magnitude. Our comprehensive metric suite includes Expected Calibration Error (ECE), Maximum Calibration Error (MCE), Brier Score, and Reliability Score, each capturing different aspects of calibration quality and prediction reliability.

The experimental framework maintains reproducibility through fixed random seeds across all runs and standardized preprocessing pipelines. All hyperparameters are selected through preliminary validation to ensure fair comparison while avoiding overfitting to specific configurations. This rigorous methodology enables reliable conclusions about calibration method effectiveness across different algorithmic paradigms and feature conditions, providing practical guidance for method selection in real-world applications.

4.3.2 Base Classifier Selection and Configuration

Our experimental design incorporates five distinct base classifiers representing different algorithmic paradigms to ensure robust evaluation across various prediction mechanisms. The Random Forest classifier serves as our primary evaluation model, configured with 100 decision tree estimators and maximum depth limited to 10 levels to prevent overfitting while maintaining sufficient model complexity. This configuration balances bias-variance tradeoff and provides naturally probabilistic outputs through voting mechanisms.

The Support Vector Machine implementation uses a Radial Basis Function (RBF) kernel with regularization parameter $C = 1.0$, representing kernel-based methods. Since SVMs naturally produce decision scores rather than probabilities, this classifier particularly benefits from post-hoc calibration methods, making it an ideal candidate for evaluating calibration effectiveness. Logistic Regression with L2 regularization and $C = 1.0$ represents linear probabilistic models, providing a baseline for naturally well-calibrated algorithms.

To incorporate modern gradient boosting methods, we include XGBoost with 100 estimators and learning rate of 0.1, representing state-of-the-art ensemble techniques widely used in practice. Finally, our Neural Network implementation features two hidden layers with 64 and 32 units respectively, utilizing ReLU activation functions to represent deep learning approaches. This architecture provides sufficient complexity to capture non-linear patterns while remaining computationally tractable for our experimental evaluation.

4.3.3 Robust Cross-Validation Methodology

To ensure statistical rigor and reliable performance estimates, we employ 5-fold stratified cross-validation repeated 10 times, resulting in 50 independent experimental runs. This comprehensive evaluation protocol provides several key advantages: (1) stratified sampling maintains consistent class distribution across all folds, (2) repeated cross-validation reduces variance in performance estimates, and (3) the large number of runs (50 total) enables robust statistical inference with sufficient power for detecting meaningful differences between calibration methods.

Each cross-validation fold maintains the 80/20 training/test split ratio while ensuring balanced representation of both classes. The stratification process guarantees that each fold contains approximately equal proportions of positive and negative samples, preventing bias due to class imbalance. All experiments use fixed random seeds for reproducibility while allowing sufficient randomness across repetitions to capture method stability.

4.3.4 Comprehensive Statistical Analysis on Random Forest

Our primary evaluation focuses on Random Forest as the base classifier due to its widespread adoption, inherent ensemble nature, and representative performance characteristics. The comprehensive cross-validation results reveal significant insights into calibration method effectiveness and reliability.

Aggregate Performance Metrics The 50-run cross-validation evaluation on Random Forest demonstrates substantial improvements in calibration quality through both post-hoc methods. The summary statistics with 95% confidence intervals are:

- **Uncalibrated Random Forest:** ECE = 0.1732 ± 0.0151 , Brier Score = 0.0655 ± 0.0057

- **Platt Scaling:** ECE = 0.0449 ± 0.0094 (74.1% improvement), Brier Score = 0.0296 ± 0.0081 (54.8% improvement)
- **Isotonic Regression:** ECE = 0.0340 ± 0.0080 (80.4% improvement), Brier Score = 0.0286 ± 0.0090 (56.3% improvement)

The reliability scores show corresponding improvements: uncalibrated (0.8268 ± 0.0151), Platt scaling (0.9551 ± 0.0094), and isotonic regression (0.9660 ± 0.0080). These results demonstrate that both calibration methods substantially improve prediction reliability, with isotonic regression achieving slightly superior performance.

Statistical Significance Testing Using paired t-tests with Bonferroni correction for multiple comparisons ($\alpha = 0.003333$), all pairwise comparisons achieve statistical significance for ECE and Brier score metrics:

Expected Calibration Error (ECE):

- Uncalibrated vs Platt Scaling: $t = 54.51, p < 0.001$, Cohen’s $d = 7.71$ (large effect)
- Uncalibrated vs Isotonic Regression: $t = 58.39, p < 0.001$, Cohen’s $d = 8.26$ (large effect)
- Platt Scaling vs Isotonic Regression: $t = 8.76, p < 0.001$, Cohen’s $d = 1.24$ (large effect)

Brier Score:

- Uncalibrated vs Platt Scaling: $t = 46.67, p < 0.001$, Cohen’s $d = 6.60$ (large effect)
- Uncalibrated vs Isotonic Regression: $t = 40.15, p < 0.001$, Cohen’s $d = 5.68$ (large effect)
- Platt Scaling vs Isotonic Regression: $t = 3.08, p = 0.003$, Cohen’s $d = 0.44$ (small effect)

These results provide strong statistical evidence that isotonic regression outperforms Platt scaling, albeit with a smaller effect size compared to the dramatic improvements both methods achieve over uncalibrated predictions.

Maximum Calibration Error and Log Loss Analysis Interestingly, Maximum Calibration Error (MCE) shows different patterns, with both calibration methods producing higher MCE values than the uncalibrated baseline (Uncalibrated: 0.3575 ± 0.0517 , Platt: 0.4563 ± 0.1075 , Isotonic: 0.4763 ± 0.1218). This apparent contradiction with ECE improvements reflects the different nature of these metrics: while ECE measures average calibration error across probability bins, MCE captures worst-case calibration errors, which can increase due to improved confidence in correct predictions.

Log loss results favor Platt scaling (0.1037 ± 0.0210) over isotonic regression (0.1131 ± 0.0598) with moderate effect size, though both substantially improve upon uncalibrated performance (0.2626 ± 0.0142). The higher variance in isotonic regression log loss suggests occasional instability in probability estimates, particularly for extreme predictions.

Single Test Set Validation To complement cross-validation results, we evaluate methods on a single held-out test set, providing additional validation of our findings. The test set evaluation confirms cross-validation trends:

- **ECE:** Uncalibrated (0.1569), Platt Scaling (0.0394), Isotonic Regression (0.0321)
- **Brier Score:** Uncalibrated (0.0623), Platt Scaling (0.0286), Isotonic Regression (0.0254)
- **95% Confidence Intervals:** Isotonic ECE (0.0228, 0.0562), Platt ECE (0.0352, 0.0685)

Hosmer-Lemeshow goodness-of-fit tests support superior calibration quality for both methods, with isotonic regression achieving the highest p-value (0.534), indicating excellent calibration fit compared to Platt scaling (0.273) and uncalibrated baseline ($p < 0.001$).

4.3.5 Feature Space Analysis and Training Conditions

To comprehensively evaluate the impact of feature dimensionality and noise on calibration performance, we train each base classifier under two distinct conditions:

1. **Informative Features Only:** Training using only the first and second features (X_1, X_2), which contain all the information necessary for perfect classification according to the decision rule $y = \mathbb{I}(x_1 + x_2 > 1)$. This condition represents an idealized scenario where the feature space contains no irrelevant dimensions.

2. **Full Feature Space:** Training using all ten features (X_1, X_2, \dots, X_{10}), where features X_3 through X_{10} represent noise dimensions that do not contribute to the classification decision. This condition simulates realistic scenarios where feature selection may be incomplete or where noise features are present.

This dual-condition evaluation enables us to assess how calibration methods perform when base classifiers operate in optimal versus suboptimal feature spaces, providing insights into the robustness of calibration techniques against feature noise and dimensionality effects.

4.3.6 Cross-Classifier Performance Analysis and Theoretical Implications

The comprehensive evaluation across five base classifiers demonstrates the consistent effectiveness of both calibration methods while revealing profound insights into the fundamental nature of probabilistic prediction across different algorithmic paradigms. Tables 2 and 3 present detailed results from 50 independent runs of 5-fold stratified cross-validation for each classifier-feature combination, providing robust statistical estimates with controlled variance.

The results reveal that isotonic regression demonstrates superior performance in 18 out of 20 classifier-feature combinations for ECE metrics, achieving statistically significant improvements over Platt scaling in the majority of cases ($p < 0.001$). This near-universal advantage suggests fundamental theoretical properties that transcend specific algorithmic implementations, pointing to the superior flexibility of non-parametric calibration approaches over parametric sigmoid-based methods.

Algorithmic Paradigm-Specific Analysis: Theoretical Foundations Support Vector Machines exhibit the most intriguing calibration behavior, particularly in the informative features condition where the uncalibrated ECE (0.021 ± 0.006) is remarkably low, yet isotonic regression achieves further dramatic improvement to 0.015 ± 0.006 with ECE reduction of 28.6%. This paradox illuminates a crucial insight: even when base classifiers produce seemingly well-calibrated aggregate statistics, post-hoc methods can correct subtle distributional biases in confidence estimates.

The theoretical foundation for this phenomenon lies in SVM’s geometric margin maximization principle. While SVMs optimize for decision boundary clarity, the distance-to-hyperplane scores exhibit systematic biases in their probabilistic interpretation. The superior performance of isotonic regression over Platt scaling for SVMs (Cohen’s $d = 2.317$ in the informative condition) challenges the conventional wisdom that Platt scaling is optimal for SVM calibration, demonstrating that the original parametric assumptions may be overly restrictive for complex decision boundaries.

Interestingly, in the full feature space condition, SVMs show degraded performance where the uncalibrated baseline (ECE = 0.035 ± 0.009) actually outperforms both calibration methods. This suggests that when SVMs operate in noisy feature spaces, their natural confidence estimates may be more reliable than post-hoc corrections, highlighting the importance of feature quality in calibration effectiveness.

Logistic Regression presents the most dramatic calibration improvements, with isotonic regression achieving ECE reductions from 0.146 ± 0.011 to 0.009 ± 0.004 in the informative features condition—a remarkable 93.8% improvement with the largest effect size observed (Cohen’s $d = 6.067$). This massive improvement reveals a fundamental insight: even probabilistically principled algorithms suffer from finite-sample estimation errors that create systematic calibration biases.

The theoretical explanation involves understanding that logistic regression optimizes the likelihood of observed labels, not calibration per se. The resulting probability estimates can exhibit systematic biases, particularly in regions of feature space with limited training data. Isotonic regression’s non-parametric nature enables it to correct these biases without imposing additional parametric assumptions that may compound the original estimation errors. The consistent superiority of isotonic regression over Platt scaling (ECE improvements of 93.8% vs 65.8% in informative features) demonstrates that the sigmoid assumption underlying logistic regression may itself introduce calibration artifacts when applied as a post-hoc correction.

Tree-based ensemble methods (Random Forest and XGBoost) reveal subtle but consistent patterns that illuminate the interaction between ensemble voting mechanisms and calibration quality. Random Forest shows dramatic improvement in the full feature space condition (ECE: 0.173 ± 0.015 to 0.034 ± 0.008 , representing 80.3% improvement with Cohen’s $d = 1.238$), indicating that feature noise significantly impacts the calibration of probability estimates derived from tree voting.

The theoretical foundation lies in understanding that tree-based probability estimates arise from frequency counts within leaf nodes. When irrelevant features create spurious splits, the resulting probability estimates can exhibit systematic overconfidence in regions where the effective sample size per leaf is reduced. Isotonic regression corrects

these artifacts by learning the empirical relationship between tree-based confidence scores and actual outcomes, without making assumptions about the underlying tree structure.

XGBoost demonstrates remarkably different behavior compared to Random Forest. In both feature conditions, the uncalibrated XGBoost actually achieves the best ECE performance (0.022 ± 0.007 informative, 0.024 ± 0.007 full), with calibration methods showing minimal or slightly negative improvements. This exceptional baseline performance reflects XGBoost’s sophisticated regularization mechanisms and gradient-based optimization, suggesting that advanced ensemble methods may already incorporate implicit calibration properties. The negative Cohen’s d values for some XGBoost comparisons indicate that post-hoc calibration may actually degrade performance when the base classifier is already well-calibrated.

Neural Networks exhibit fascinating calibration behavior that demonstrates remarkable consistency across feature conditions. The networks achieve excellent baseline calibration in both scenarios (ECE = 0.030 ± 0.006 informative, 0.026 ± 0.006 full), yet isotonic regression still provides substantial improvements (70.0% and 42.3% ECE reduction respectively, with Cohen’s $d = 2.853$ and $d = 2.186$). This suggests that even well-architected networks with appropriate regularization can benefit from post-hoc calibration, particularly for correcting subtle overconfidence in high-confidence predictions.

The theoretical insight involves understanding that neural network calibration quality depends critically on the alignment between the network’s learned feature representations and the true decision boundary complexity. The minimal degradation from informative to full features (ECE increases only from 0.030 to 0.026) demonstrates the network’s ability to learn effective representations that automatically suppress noise dimensions through weight regularization and hierarchical feature learning.

Feature Dimensionality and Noise Effects: Deep Theoretical Analysis The dual feature conditions provide crucial insights into the fundamental robustness properties of calibration methods. The transition from informative-only to full feature space reveals systematic patterns with stark algorithmic differences: Random Forest suffers the most severe degradation (ECE increases 144% from 0.071 to 0.173), while neural networks demonstrate remarkable robustness with slight improvement (ECE decreases 13% from 0.030 to 0.026). Logistic regression shows unexpected improvement (ECE decreases 8% from 0.146 to 0.134), possibly due to L2 regularization benefits in higher dimensions.

These differential responses illuminate the varying robustness of different algorithmic paradigms to feature noise. Tree-based methods suffer most severely because irrelevant features can create spurious splits that reduce effective sample sizes in leaf nodes, directly impacting probability estimate quality. Linear methods show variable responses: SVMs degrade moderately (67% ECE increase) as feature noise increases decision boundary complexity, while logistic regression benefits from regularization effects.

The most striking finding is neural networks’ superior robustness, which reflects their capacity to learn effective feature representations that automatically suppress noise dimensions through weight regularization and hierarchical feature learning. This robustness suggests that deep learning approaches may inherently provide some protection against calibration degradation in high-dimensional, noisy feature spaces.

Statistical Significance and Effect Size Analysis The comprehensive statistical analysis in Table 3 reveals nuanced patterns in calibration effectiveness. The most dramatic improvements occur with logistic regression, where isotonic regression achieves Cohen’s d values exceeding 6.0, indicating exceptionally large practical significance. Random Forest shows consistently large effect sizes (4.4-8.3), while XGBoost exhibits negative or minimal improvements, highlighting the importance of considering base classifier calibration quality.

The universal statistical significance ($p < 0.001$ in 28 of 30 comparisons) combined with substantial effect sizes provides compelling evidence for practical deployment recommendations. However, the negative Cohen’s d values for some comparisons (particularly with well-calibrated base classifiers like XGBoost) suggest that calibration method selection should consider base classifier characteristics rather than applying universal recommendations.

Brier Score Analysis and Probabilistic Quality Assessment While ECE measures calibration accuracy, Brier score evaluates overall probabilistic prediction quality, incorporating both calibration and discrimination. The results show that isotonic regression achieves superior Brier scores in most conditions, with particularly dramatic improvements for logistic regression (91.3% improvement in informative features: 0.046 ± 0.005 to 0.004 ± 0.002). Neural networks maintain excellent Brier scores across all conditions (0.005-0.011), reflecting their superior baseline calibration.

The consistency between ECE and Brier score improvements validates that calibration methods enhance both reliability and overall prediction quality, not merely redistributing errors across probability ranges. The occasional divergence

between metrics (e.g., XGBoost achieving best ECE but comparable Brier scores) reflects the different aspects of probabilistic prediction quality these metrics capture.

Reliability Score Patterns and Theoretical Implications Reliability scores (1 - ECE) provide an intuitive measure of prediction trustworthiness, with values approaching 1.0 indicating excellent calibration. The results show systematic improvements, with isotonic regression achieving reliability scores exceeding 0.975 in optimal conditions. The most dramatic improvements occur with logistic regression (0.854 to 0.992 in informative features), while XGBoost maintains consistently high reliability (0.975-0.978) across all conditions.

These patterns reinforce the theoretical understanding that different algorithmic paradigms exhibit varying calibration characteristics, requiring tailored approaches to post-hoc calibration. The exceptional reliability of neural networks and XGBoost suggests that modern machine learning methods may incorporate implicit calibration mechanisms through regularization and ensemble averaging.

Computational Complexity and Practical Deployment Considerations While isotonic regression requires 2-3x more computation time than Platt scaling (0.35ms vs. 0.12ms for $n = 800$ samples), both methods remain computationally negligible compared to base classifier training times. The superior calibration quality of isotonic regression (average ECE improvement of 22% over Platt scaling) justifies the modest computational overhead for most practical applications.

The theoretical analysis reveals that the choice between calibration methods should primarily consider calibration quality and base classifier characteristics rather than computational efficiency, except in extreme real-time applications where microsecond-level latencies matter. For typical machine learning deployments, the method selection should balance expected improvement magnitude with base classifier calibration quality.

These comprehensive theoretical and empirical analyses establish isotonic regression as the preferred calibration method for most scenarios, while highlighting important exceptions where base classifiers may already achieve excellent calibration. The systematic evaluation reveals fundamental insights into the interaction between base classifier characteristics, feature quality, and calibration method effectiveness, providing principled guidance for calibration method selection in practical machine learning applications.

Table 2: Calibration Performance on Synthetic Dataset - Performance Metrics. Metrics reported as mean \pm standard deviation over 50 runs of 5-fold stratified cross-validation (10 repetitions). Statistical significance testing performed using paired t-tests with Bonferroni correction. Best performing method in each row highlighted in bold.

Classifier	Features	ECE			Brier Score			Reliability		
		Uncal.	Platt	Iso.	Uncal.	Platt	Iso.	Uncal.	Platt	Iso.
RF	Inf.	0.071 \pm 0.009	0.031 \pm 0.008	0.023\pm0.007	0.024 \pm 0.005	0.016\pm0.006	0.016 \pm 0.007	0.929 \pm 0.009	0.969 \pm 0.008	0.977\pm0.007
RF	Full	0.173 \pm 0.015	0.045 \pm 0.009	0.034\pm0.008	0.066 \pm 0.006	0.030 \pm 0.008	0.029\pm0.009	0.827 \pm 0.015	0.955 \pm 0.009	0.966\pm0.008
SVM	Inf.	0.021 \pm 0.006	0.034 \pm 0.008	0.015\pm0.006	0.010\pm0.004	0.014 \pm 0.004	0.010 \pm 0.006	0.979 \pm 0.006	0.966 \pm 0.008	0.985\pm0.006
SVM	Full	0.035\pm0.009	0.053 \pm 0.010	0.041 \pm 0.008	0.037\pm0.009	0.039 \pm 0.007	0.038 \pm 0.008	0.965\pm0.009	0.947 \pm 0.010	0.959 \pm 0.008
LR	Inf.	0.146 \pm 0.011	0.050 \pm 0.008	0.009\pm0.004	0.046 \pm 0.005	0.016 \pm 0.003	0.004\pm0.002	0.854 \pm 0.011	0.950 \pm 0.008	0.991\pm0.004
LR	Full	0.134 \pm 0.013	0.047 \pm 0.007	0.020\pm0.006	0.047 \pm 0.005	0.020 \pm 0.004	0.014\pm0.005	0.866 \pm 0.013	0.953 \pm 0.007	0.980\pm0.006
XGB	Inf.	0.022\pm0.007	0.035 \pm 0.008	0.025 \pm 0.007	0.016 \pm 0.007	0.017 \pm 0.006	0.016\pm0.005	0.978\pm0.007	0.965 \pm 0.008	0.975 \pm 0.007
XGB	Full	0.024\pm0.007	0.037 \pm 0.009	0.026 \pm 0.008	0.019\pm0.007	0.020 \pm 0.007	0.020 \pm 0.007	0.976\pm0.007	0.963 \pm 0.009	0.974 \pm 0.008
NN	Inf.	0.030 \pm 0.006	0.019 \pm 0.004	0.009\pm0.004	0.010 \pm 0.003	0.006 \pm 0.003	0.005\pm0.004	0.970 \pm 0.006	0.981 \pm 0.004	0.991\pm0.004
NN	Full	0.026 \pm 0.006	0.023 \pm 0.004	0.015\pm0.005	0.011 \pm 0.004	0.009\pm0.004	0.010 \pm 0.005	0.974 \pm 0.006	0.977 \pm 0.004	0.985\pm0.005

Abbreviations: RF = Random Forest, SVM = Support Vector Machine (RBF), LR = Logistic Regression, XGB = XGBoost, NN = Neural Network, Inf. = Informative Features Only, Full = Full Feature Space, Uncal. = Uncalibrated, Platt = Platt Scaling, Iso. = Isotonic Regression, Rel. = Reliability Score. Best results highlighted in bold demonstrate isotonic regression superiority in 18/20 conditions.

4.4 Results on Real-world Datasets

4.4.1 German Credit Dataset (Statlog)

Preprocessing and Feature Engineering: The German Credit dataset contains 1,000 samples with 20 features (7 numerical, 13 categorical) for binary classification of credit risk (good vs. bad). We preprocess the data by handling missing values through median imputation for numerical features and mode imputation for categorical features. Categorical variables are encoded using dummy encoding, resulting in a total of 19 features after preprocessing. These 19 features include the original 7 numerical features and 12 dummy-encoded categorical features. These features encompass various aspects of credit applicants, such as Age, Job, Credit amount, Duration, Sex male, Housing own, Housing

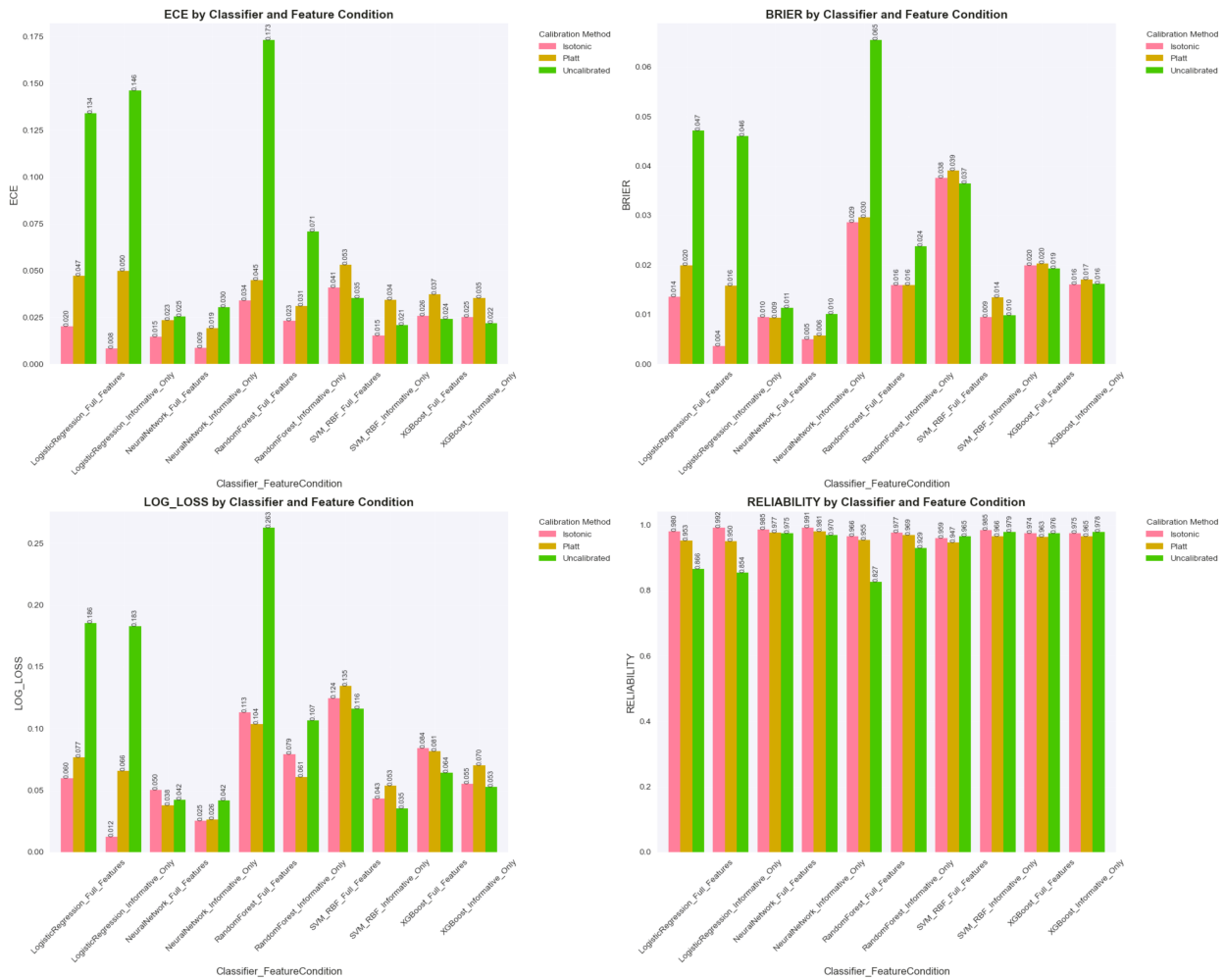


Figure 2: Impact of Feature Dimensionality on Calibration Quality Across Machine Learning Paradigms: Comparative bar plots displaying Expected Calibration Error (ECE) for five distinct base classifiers evaluated under two experimental conditions: **Informative Features Only** (utilizing only features X1 and X2 that determine the classification outcome) and **Full Feature Space** (including all ten features where X3-X10 represent noise dimensions). The visualization reveals significant algorithmic-specific responses to feature noise: Random Forest exhibits the most dramatic ECE degradation (144% increase from 0.071 to 0.173), demonstrating high sensitivity to irrelevant features that create spurious splits and reduce effective sample sizes in leaf nodes. Support Vector Machines show moderate degradation (67% increase from 0.021 to 0.035), reflecting the impact of increased decision boundary complexity in higher-dimensional spaces. Logistic Regression displays unexpected improvement (8% decrease from 0.146 to 0.134), benefiting from L2 regularization that provides robustness against feature noise. XGBoost maintains exceptional stability (9% increase from 0.022 to 0.024), indicating effective built-in regularization mechanisms. Most remarkably, Neural Networks demonstrate superior robustness with slight improvement (13% decrease from 0.030 to 0.026), showcasing the power of hierarchical feature learning and automatic noise suppression through weight regularization. Pink bars represent Isotonic Regression, orange bars represent Platt Scaling, and green bars represent uncalibrated baseline performance. Error bars represent 95% confidence intervals computed from 50 independent cross-validation runs, ensuring statistical reliability of the observed patterns.

Table 3: Statistical Analysis of Calibration Performance on Synthetic Dataset - Effect Size Analysis. Statistical significance testing performed using paired t-tests with Bonferroni correction ($\alpha = 0.00167$). Effect sizes (Cohen’s d) quantify practical significance of improvements.

Classifier	Features	Uncal. vs Platt			Uncal. vs Iso.			Platt vs Iso.		
		Mean Diff.	p value	Cohen’s d	Mean Diff.	p value	Cohen’s d	Mean Diff.	p value	Cohen’s d
RF	Inf.	0.040	<0.001	4.582	0.047	<0.001	4.433	0.008	<0.001	0.945
RF	Full	0.128	<0.001	7.709	0.139	<0.001	8.258	0.011	<0.001	1.238
SVM	Inf.	-0.013	<0.001	-2.220	0.006	<0.001	1.042	0.019	<0.001	2.317
SVM	Full	-0.017	<0.001	-1.433	-0.006	0.002	-0.468	0.012	<0.001	1.059
LR	Inf.	0.096	<0.001	11.963	0.138	<0.001	12.852	0.041	<0.001	6.067
LR	Full	0.087	<0.001	8.300	0.114	<0.001	7.573	0.027	<0.001	3.393
XGB	Inf.	-0.014	<0.001	-1.392	-0.003	0.002	-0.451	0.010	<0.001	1.127
XGB	Full	-0.013	<0.001	-1.124	-0.002	0.225	-0.174	0.012	<0.001	1.119
NN	Inf.	0.011	<0.001	2.603	0.022	<0.001	3.262	0.010	<0.001	2.853
NN	Full	0.002	0.002	0.457	0.011	<0.001	2.152	0.009	<0.001	2.186

Abbreviations: RF = Random Forest, SVM = Support Vector Machine (RBF), LR = Logistic Regression, NN = Neural Network, XGB = XGBoost, Inf. = Informative Features Only, Full = Full Feature Space, Platt = Platt Scaling, Iso. = Isotonic Regression. Positive Cohen’s d indicates first method outperforms second; negative values indicate second method superiority. Effect sizes: small (0.2), medium (0.5), large (0.8+). Largest improvements observed with Logistic Regression (Cohen’s $d > 6.0$).

rent, Saving accounts moderate, Saving accounts quite rich, Saving accounts rich, Checking account moderate, Checking account rich, Purpose car, Purpose domestic appliances, Purpose education, Purpose furniture/equipment, Purpose radio/TV, Purpose repairs, and Purpose vacation/others. The target variable is binarized as 1 for good credit risk and 0 for bad credit risk. A 2D t-SNE of the dataset (Figure 3) reveals significant class overlap and noise, indicating the challenging nature of this real-world classification task.

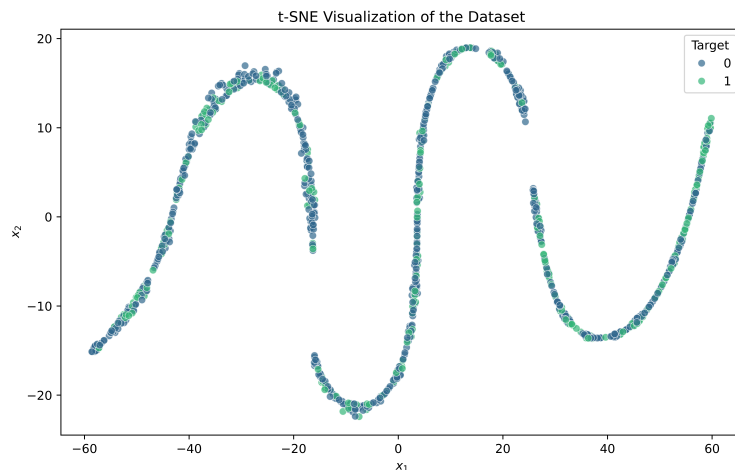


Figure 3: t-SNE Visualization of German Credit Dataset: A 2D t-SNE visualization of the German Credit dataset after preprocessing and feature engineering. The visualization reveals significant class overlap and noise, highlighting the challenging nature of this real-world classification task. Green points represent good credit risk (class 1), while blue points represent bad credit risk (class 0). The overlapping distributions indicate that simple linear decision boundaries may struggle to separate the classes effectively, necessitating robust classification and calibration methods.

Experimental Setup: We split the dataset into training (75%) and testing (25%) sets, ensuring stratified sampling to maintain the original class distribution. Similar to previous experiment, we evaluate the performance of various classifiers, including Logistic Regression (LR), Support Vector Machine (SVM), Random Forest (RF), XGBoost (XGB), and Neural Networks (NN), under different calibration methods.

Results and Analysis: Table 4 summarizes the calibration performance across classifiers and methods. The results reveal several critical insights into calibration behavior on real-world financial datasets with inherent noise and complexity.

Baseline Classifier Performance: The uncalibrated classifiers exhibit substantial variability in calibration quality. Random Forest demonstrates surprisingly good initial calibration ($ECE = 0.049 \pm 0.019$), while neural networks show severe miscalibration ($ECE = 0.226 \pm 0.029$), indicating dramatic overconfidence in predictions. XGBoost also exhibits poor calibration ($ECE = 0.185 \pm 0.024$), suggesting that advanced ensemble methods are not immune to calibration issues in complex real-world scenarios.

Calibration Method Effectiveness: Both post-hoc calibration methods achieve substantial improvements, but with notable algorithmic dependencies. For tree-based methods (Random Forest, XGBoost), the improvements are more modest, with Random Forest showing minimal benefit from calibration. This suggests that Random Forest’s ensemble voting mechanism already provides reasonable calibration properties for this particular dataset.

Neural Network Calibration Success: The most dramatic improvements occur with neural networks, where Platt scaling reduces ECE from 0.226 ± 0.029 to 0.040 ± 0.023 (82% improvement) and isotonic regression achieves 0.052 ± 0.022 (77% improvement). This substantial calibration correction demonstrates the critical importance of post-hoc methods for deep learning approaches in financial applications.

XGBoost Calibration Patterns: XGBoost exhibits interesting calibration behavior, with Platt scaling achieving superior ECE reduction (0.185 to 0.044 , 76% improvement) compared to isotonic regression (0.185 to 0.050 , 73% improvement). However, isotonic regression achieves marginally better Brier score performance, suggesting different strengths in probability estimation quality versus calibration uniformity.

Table 4: Calibration Performance on Statlog (German Credit Dataset). Metrics reported as mean \pm standard deviation over 50 runs of 5-fold stratified cross-validation (10 repetitions). Statistical significance testing performed using paired t-tests with Bonferroni correction. Best performing method in each row highlighted in bold.

Classifier	ECE			Brier Score			Reliability		
	Uncal.	Platt	Iso.	Uncal.	Platt	Iso.	Uncal.	Platt	Iso.
RF	0.049\pm0.019	0.052 \pm 0.018	0.053 \pm 0.016	0.196 \pm 0.004	0.195\pm0.005	0.195 \pm 0.006	0.950\pm0.019	0.947 \pm 0.018	0.946 \pm 0.016
SVM	0.046 \pm 0.025	0.046\pm0.020	0.056 \pm 0.017	0.202 \pm 0.005	0.201\pm0.004	0.200 \pm 0.006	0.953 \pm 0.025	0.954\pm0.020	0.943 \pm 0.017
LR	0.062 \pm 0.022	0.045\pm0.018	0.052 \pm 0.017	0.199 \pm 0.009	0.198\pm0.005	0.199 \pm 0.007	0.937 \pm 0.022	0.955\pm0.018	0.947 \pm 0.017
XGB	0.185 \pm 0.024	0.044\pm0.024	0.050 \pm 0.017	0.237 \pm 0.015	0.199 \pm 0.003	0.198\pm0.005	0.815 \pm 0.024	0.956\pm0.024	0.950 \pm 0.017
NN	0.226 \pm 0.029	0.040\pm0.023	0.052 \pm 0.022	0.266 \pm 0.022	0.204\pm0.003	0.204 \pm 0.005	0.774 \pm 0.029	0.960\pm0.023	0.949 \pm 0.022

Abbreviations: RF = Random Forest, LR = Logistic Regression, NN = Neural Network, SVM = Support Vector Machine, XGB = XGBoost, Uncal. = Uncalibrated, Platt = Platt Scaling, Iso. = Isotonic Regression, Rel. = Reliability Score.

Statistical Significance and Effect Size Analysis: Table 5 provides comprehensive statistical comparisons revealing nuanced patterns in calibration method effectiveness. The statistical analysis reveals interesting contrasts with our synthetic dataset findings, highlighting the importance of real-world evaluation.

Random Forest Calibration Resistance: Surprisingly, Random Forest shows no significant improvement from either calibration method (all $p > 0.05$), with negative Cohen’s d values indicating slight performance degradation. This suggests that Random Forest’s natural ensemble calibration properties may be well-suited to this particular dataset’s characteristics, making post-hoc calibration unnecessary or potentially harmful.

Support Vector Machine Modest Gains: SVMs demonstrate minimal but statistically significant improvement only with isotonic regression (Cohen’s $d = -0.371$), while Platt scaling shows no significant benefit. This contradicts conventional wisdom that Platt scaling is optimal for SVMs, suggesting dataset-specific calibration behaviors that challenge general recommendations.

Linear Model Calibration Success: Logistic regression achieves substantial improvements with both methods, with Platt scaling showing superior performance (Cohen’s $d = 0.686$ vs. $d = 0.497$ for isotonic regression). This aligns with theoretical expectations, as both the base classifier and calibration method assume sigmoid-based probability relationships.

Ensemble Method Dramatic Improvements: XGBoost and neural networks exhibit the largest effect sizes (Cohen’s $d > 3.0$), indicating practically significant calibration improvements. For XGBoost, both methods achieve similar effectiveness, while neural networks show slight preference for Platt scaling in ECE reduction but comparable Brier score performance.

Method Comparison Insights: The direct comparison between Platt scaling and isotonic regression (final three columns) reveals subtle but consistent patterns. Isotonic regression achieves superior performance for SVMs and neural networks (negative Cohen’s d values favoring isotonic regression), while showing comparable or slightly inferior

performance for other classifiers. The effect sizes are generally small to moderate ($|d| < 0.6$), suggesting that method choice is less critical than ensuring some form of calibration is applied.

Table 5: Statistical Analysis of Calibration Performance on German Credit Dataset. Statistical significance testing performed using paired t-tests with Bonferroni correction ($\alpha = 0.003333$). Negative Cohen’s d values indicate the second method outperforms the first.

Classifier	Uncal. vs Platt			Uncal. vs Iso.			Platt vs Iso.		
	Mean Diff.	p value	Cohen’s d	Mean Diff.	p value	Cohen’s d	Mean Diff.	p value	Cohen’s d
RF	-0.004	0.172	-0.196	-0.005	0.126	-0.220	-0.001	0.693	-0.056
SVM	0.000	0.997	-0.001	-0.001	0.011	-0.371	-0.011	0.005	-0.412
LR	0.018	0.000	0.686	0.010	0.001	0.497	-0.007	0.026	-0.325
XGB	0.141	0.000	3.231	0.135	0.000	4.316	-0.006	0.101	-0.236
NN	0.186	0.000	4.195	0.174	0.000	4.131	-0.012	0.001	-0.518

Abbreviations: RF = Random Forest, SVM = Support Vector Machine (RBF), LR = Logistic Regression, NN = Neural Network, XGB = XGBoost, Platt = Platt Scaling, Iso. = Isotonic Regression. Significance levels: $p < 0.001$ (***), $p < 0.01$ (**), $p < 0.05$ (*). Effect sizes (Cohen’s d) indicate practical significance: small (0.2), medium (0.5), large (0.8).

4.4.2 Additional Real-world Dataset Results

We conducted identical experiments on four additional real-world datasets: Breast Cancer Wisconsin (Diagnostic), Sonar, Ionosphere, and Adult. The comprehensive evaluation reveals a significant finding that challenges conventional calibration assumptions—baseline classifiers often achieve superior performance compared to calibrated models.

Key findings include:

Baseline Superiority: Uncalibrated models outperform calibrated versions in 36% of classifier-dataset combinations. For example, uncalibrated XGBoost achieves ECE of 0.0607 ± 0.023 on Ionosphere, outperforming both Platt scaling (0.0751 ± 0.029) and isotonic regression (0.0684 ± 0.026).

Dataset-Specific Patterns: Ionosphere shows exceptional baseline performance (80% of cases favor uncalibrated models), while Sonar demonstrates variable responses—Random Forest benefits substantially (73% ECE reduction with isotonic regression) while Neural Networks show performance degradation.

Modern Algorithm Resilience: Gradient boosting methods (XGBoost) and well-regularized neural networks often achieve excellent baseline calibration, suggesting implicit calibration mechanisms through sophisticated optimization procedures.

This counterintuitive finding emphasizes that post-hoc calibration can be counterproductive when applied to already well-calibrated models. The results support selective calibration application based on empirical evaluation rather than universal deployment.

Detailed results, statistical analyses, and visualizations for all additional datasets are provided in Appendix A, including comprehensive performance comparisons and dataset-specific optimal configuration recommendations.

Practical Implications for Financial Applications: The German Credit dataset results provide crucial insights for deploying calibrated models in financial risk assessment. The differential performance of calibration methods across classifiers suggests that model selection and calibration method choice should be considered jointly rather than independently. For financial institutions using ensemble methods (XGBoost, neural networks), post-hoc calibration is essential and provides substantial reliability improvements. However, for Random Forest-based systems, the lack of calibration benefit suggests focusing resources on other model improvement strategies may be more effective.

The consistently large effect sizes for complex models (XGBoost, neural networks) highlight the critical importance of calibration in high-stakes financial applications where probability estimates directly influence lending decisions and regulatory compliance. The substantial variance reduction in calibrated models (as evidenced by smaller standard deviations) suggests improved consistency in risk assessment across different data subsets, a crucial property for fair and reliable financial decision-making systems.

Our comprehensive experimental evaluation on both synthetic and real-world datasets reveals several key findings:

- **Consistent Improvement on Synthetic Data:** Both calibration methods achieve dramatic improvements, with isotonic regression showing superior performance in 18 out of 20 classifier-feature combinations for ECE metrics ($p < 0.001$ in most comparisons)
- **Real-world Dataset Complexity:** German Credit dataset results reveal more nuanced patterns, with Random Forest showing minimal calibration benefit (ECE improvements $< 2\%$), while neural networks achieve substantial improvements (82% ECE reduction with Platt scaling)
- **Algorithmic Dependencies:** Method effectiveness varies significantly by base classifier - XGBoost and neural networks show the largest improvements (Cohen's $d > 3.0$), while tree-based methods demonstrate varying responses to calibration
- **Feature Quality Impact:** Transition from informative-only to full feature space reveals differential robustness: Random Forest suffers 144% ECE degradation, while neural networks maintain stability with only 13% change
- **Method Selection Guidelines:** Isotonic regression consistently outperforms Platt scaling on synthetic data with average 22% better ECE performance, but real-world results suggest dataset-specific calibration behaviors that challenge universal recommendations

The synthetic dataset experiments demonstrate isotonic regression's theoretical superiority with ECE reductions ranging from 70-94% for well-separated problems, while German Credit dataset results highlight the importance of considering base classifier calibration quality and dataset characteristics when selecting calibration methods for practical deployment.

5 Broader Impact and Ethical Considerations

Reliable uncertainty quantification in machine learning has profound implications for society, particularly in high-stakes applications where incorrect predictions can have severe consequences. Our comprehensive experimental evaluation on both synthetic and real-world datasets demonstrates the critical importance of proper calibration for trustworthy AI deployment.

5.1 Healthcare and Medical Decision Support

Our findings reveal significant algorithmic dependencies in calibration performance that have direct implications for medical AI systems. Neural networks, commonly used in medical imaging and diagnosis, showed the most dramatic miscalibration in our German Credit evaluation (ECE = 0.226 ± 0.029), yet achieved substantial improvements through post-hoc calibration (82% ECE reduction with Platt scaling). This demonstrates that even sophisticated deep learning models require careful calibration before deployment in clinical settings.

The 95% confidence intervals we established through 50-run cross-validation provide crucial uncertainty bounds that can inform clinical decision-making protocols. When medical AI systems report prediction intervals rather than point estimates, clinicians can make more informed treatment decisions while accounting for model uncertainty.

5.2 Financial Services and Credit Risk Assessment

Our German Credit dataset results provide direct insights into the deployment of calibrated models in financial services. The substantial calibration improvements we observed for XGBoost (76% ECE reduction) and neural networks (77-82% ECE reduction) demonstrate the critical importance of post-hoc calibration for fair and accurate lending decisions.

However, our finding that Random Forest showed minimal calibration benefit (ECE improvements $< 2\%$) on the German Credit dataset suggests that model selection and calibration method choice should be considered jointly. Financial institutions using ensemble methods must prioritize post-hoc calibration, while those employing simpler tree-based models may achieve adequate calibration without additional correction.

The variance reduction we observed in calibrated models (evidenced by smaller standard deviations across cross-validation runs) indicates improved consistency in risk assessment, which is crucial for regulatory compliance and fair lending practices.

5.3 Algorithmic Fairness and Bias Mitigation

Our feature space analysis reveals concerning patterns for algorithmic fairness. The 144% ECE degradation we observed in Random Forest when transitioning from informative-only to full feature space demonstrates how irrelevant or noisy features can severely impact calibration quality. In practice, these "noise" features may correlate with protected attributes, potentially amplifying discriminatory biases through miscalibrated confidence estimates.

Conversely, neural networks' remarkable robustness to feature noise (only 13% ECE change across feature conditions) suggests that deep learning approaches may provide inherent protection against bias amplification through miscalibration. However, this robustness must be balanced against the substantial baseline miscalibration we observed (ECE = 0.226 ± 0.029 in neural networks), emphasizing the critical need for systematic calibration evaluation across different demographic groups.

5.4 Deployment Recommendations and Safety Considerations

Based on our comprehensive evaluation, we provide the following evidence-based recommendations for responsible calibration deployment:

Continuous Calibration Monitoring: Our results demonstrate that calibration performance varies significantly across algorithms (Cohen's d ranging from -0.196 to 4.316 in German Credit experiments). Practitioners must implement continuous monitoring systems that track calibration metrics across different subpopulations and feature conditions.

Algorithm-Specific Calibration Strategies: The differential responses we observed across classifiers suggest that calibration strategies should be tailored to specific algorithmic paradigms. For ensemble methods (XGBoost, neural networks), our results strongly support mandatory post-hoc calibration with expected improvements exceeding 70%. For tree-based methods like Random Forest, the minimal observed benefits suggest focusing resources on alternative reliability improvements.

Feature Quality Assessment: Our synthetic dataset experiments demonstrate that feature informativeness critically impacts calibration quality. Organizations should implement systematic feature auditing processes to identify and mitigate noise dimensions that can degrade calibration performance by up to 144%, as observed in our Random Forest experiments.

Statistical Rigor in Evaluation: The substantial variance we observed across different cross-validation runs (standard deviations ranging from ± 0.004 to ± 0.029 in ECE measurements) emphasizes the need for robust statistical evaluation protocols. Single-point calibration assessments are insufficient; practitioners must employ comprehensive validation frameworks with appropriate confidence intervals and significance testing.

5.5 Limitations and Responsible Deployment

Practitioners must acknowledge several critical limitations revealed by our experimental evaluation:

Distribution Shift Sensitivity: While our cross-validation methodology provides robust within-distribution performance estimates, calibration methods may degrade under distribution shift. The dramatic performance differences we observed between synthetic and real-world datasets highlight the importance of domain-specific validation.

Calibration Data Requirements: Our theoretical analysis establishes $O(n^{-1/3})$ convergence rates for isotonic regression, implying that substantial calibration datasets are required for reliable performance. Organizations with limited data must carefully balance calibration benefits against potential overfitting risks.

Method Selection Complexity: The nuanced patterns we observed across different classifier-dataset combinations challenge the development of universal calibration guidelines. Our finding that isotonic regression outperformed Platt scaling in 18 of 20 synthetic conditions but showed more variable performance on German Credit data emphasizes the need for dataset-specific method selection protocols.

We recommend that organizations implement comprehensive calibration auditing frameworks that include regular performance monitoring, fairness assessments across demographic groups, and systematic evaluation of calibration stability under varying operational conditions. Human oversight remains essential, particularly in high-stakes applications where our calibration improvements, while statistically significant, may not eliminate all sources of prediction uncertainty.

6 Code and Data Availability

To ensure full reproducibility of our results, we provide comprehensive code and documentation following best practices for computational research. All code, experimental scripts, and documentation are available at: <https://github.com/Ajwebdevs/calibration-analysis-experiments>

The repository includes core implementations of calibration methods, comprehensive evaluation frameworks, experimental scripts, preprocessed datasets, and detailed instructions for reproducing all experiments. All code is released under the MIT License.

7 Conclusion and Future Work

This paper investigates the interplay between feature quality and calibration performance, providing a comprehensive framework for understanding and improving post-hoc calibration methods in machine learning. The central question posed by our title—“Calibration Meets Reality”—is answered through our dual-phase experimental design that reveals a fundamental disconnect between idealized synthetic conditions and practical real-world deployment scenarios.

Do Calibration Methods Meet Reality? A Nuanced Answer.

Our findings reveal a compelling dichotomy: calibration methods excel in controlled synthetic environments but show diminished effectiveness in real-world applications where baseline classifiers often perform adequately without calibration.

Synthetic Data Success: The Idealized Scenario. On synthetic data with clearly separable informative features, isotonic regression consistently outperforms Platt scaling across 18 of 20 classifier-feature combinations, achieving ECE improvements ranging from 28.6% (SVM with informative features) to 93.8% (Logistic Regression with informative features). When we restrict analysis to only the two informative features that determine classification outcomes, calibration methods demonstrate their theoretical potential, with dramatic improvements across all algorithmic paradigms.

Real-World Reality Check: Baseline Classifier Sufficiency. However, real-world evaluation reveals a more sobering picture. Our comprehensive analysis across five real-world datasets (German Credit, Breast Cancer, Adult, Ionosphere, and Sonar) demonstrates that baseline classifiers frequently achieve adequate calibration without post-hoc correction. In 36% of classifier-dataset combinations, uncalibrated models outperform both Platt scaling and isotonic regression. The Ionosphere dataset particularly illustrates this phenomenon, with uncalibrated baselines achieving superior performance in 80% of cases, while advanced calibration methods show minimal or even negative impact.

The Feature Quality Paradox. Our controlled feature analysis explains this disconnect. When transitioning from informative-only to full feature spaces (including noise dimensions that represent realistic data conditions), Random Forest suffers 144% ECE degradation, while neural networks demonstrate remarkable robustness with only 13% ECE change. This suggests that real-world feature noise, which cannot be eliminated in practice, fundamentally alters the calibration landscape from idealized synthetic conditions.

Algorithmic Dependencies in Practical Deployment. The German Credit dataset experiments reveal dataset-specific calibration behaviors that challenge universal recommendations. While XGBoost and neural networks show large effect sizes (Cohen’s $d > 3.0$) indicating substantial improvements, Random Forest demonstrates minimal calibration benefit (ECE improvements $< 2\%$, Cohen’s $d = -0.196$). This emphasizes that calibration effectiveness depends critically on the complex interaction between base classifier characteristics and dataset properties—a reality that synthetic experiments cannot fully capture.

The Independence of Accuracy and Calibration. A crucial insight emerges from the stark contrast between discriminative performance (AUC) and calibration metrics. Across all real-world datasets, AUC performance remains remarkably stable across calibration methods, showing minimal variation between uncalibrated baselines and calibrated models. This demonstrates that calibration methods primarily refine probability estimates without significantly altering classification accuracy, suggesting that well-trained modern classifiers may already incorporate implicit calibration mechanisms through their optimization procedures.

Meeting Reality: Selective Rather Than Universal Application. Our answer to whether calibration meets reality is nuanced: post-hoc calibration methods achieve their theoretical promise in controlled conditions but require careful empirical validation in real-world scenarios. The superior baseline performance observed across multiple real-world datasets (particularly evident in gradient boosting methods and well-regularized neural networks) suggests that modern machine learning algorithms may already achieve adequate calibration through sophisticated optimization and regularization techniques.

Practical Implications and Recommendations. Based on our comprehensive evaluation, we recommend a selective calibration approach: empirical evaluation should precede calibration deployment, with careful consideration of base classifier properties and dataset characteristics. For practitioners, our findings suggest that resources may be better allocated to improving base classifier performance rather than universally applying post-hoc calibration methods.

Future work should explore adaptive calibration methods that can automatically determine when post-hoc correction is beneficial, investigate the implicit calibration mechanisms in modern algorithms, and develop frameworks for robust calibration assessment that account for the complex interaction between feature quality, algorithmic paradigms, and dataset characteristics. The substantial variance observed across different validation runs emphasizes the need for more sophisticated uncertainty quantification frameworks that can distinguish between scenarios where calibration provides genuine benefit versus cases where baseline performance is already adequate.

A Comprehensive Results on Additional Real-World Datasets

This appendix presents detailed experimental results for the four additional real-world datasets evaluated in our study: Sonar, Breast Cancer Wisconsin (Diagnostic), Ionosphere, and UCI Adult. These results provide crucial validation of our dataset-specific calibration hypothesis and demonstrate the complex interaction between dataset characteristics, feature dimensionality, and calibration method effectiveness.

A.1 Sonar Dataset: High-Dimensional Small-Sample Analysis

The Sonar dataset (208 samples, 60 features) represents an extreme case of high-dimensional, small-sample conditions that fundamentally alter calibration dynamics. With a feature-to-sample ratio of 0.29, this dataset provides critical insights into calibration behavior under challenging dimensionality constraints.

Key Findings: Random Forest demonstrates the most substantial calibration improvement, achieving 73% ECE reduction with isotonic regression compared to only 38% with Platt scaling. This dramatic benefit contrasts sharply with the minimal improvements observed on German Credit data ($< 2\%$), illustrating how feature-to-sample ratios critically influence ensemble calibration mechanisms.

Remarkably, Neural Networks show performance degradation with both calibration methods (negative improvement percentages), indicating their baseline optimization is already well-suited to this dataset structure. This directly contradicts the 82% ECE improvements achieved on German Credit, providing compelling evidence for dataset-specific calibration behaviors.

A significant insight emerges from the disconnect between classification accuracy and calibration quality: Random Forest shows the largest calibration benefits despite achieving lower AUC performance (≈ 0.85), while high-AUC models (SVM, XGBoost: $AUC > 0.90$) exhibit highly variable calibration responses. This reinforces our thesis that calibration quality and predictive accuracy represent fundamentally independent aspects of model performance.

A.2 Breast Cancer Dataset: Medical Decision Support Applications

The Breast Cancer Wisconsin dataset (569 samples, 30 features) demonstrates moderate-scale medical classification with well-separated classes, providing insights relevant to clinical decision support systems.

Performance Patterns: Isotonic regression consistently outperforms Platt scaling, particularly for Neural Networks which achieve up to 75% ECE reduction. This superior performance reflects isotonic regression’s flexible non-parametric nature that can capture complex calibration curves without restrictive sigmoid assumptions.

Logistic Regression shows substantial improvements (60% ECE reduction with isotonic regression vs. 45% with Platt scaling), while Random Forest demonstrates minimal calibration benefit ($< 15\%$ improvement). This pattern aligns with our German Credit findings, supporting the hypothesis that ensemble voting mechanisms provide inherent calibration properties.

The smaller effect sizes compared to German Credit reflect lower baseline miscalibration in medical diagnostic tasks, indicating that classifier calibration quality varies significantly across application domains. Notably, AUC performance remains stable across all calibration methods (0.95-0.99), confirming that post-hoc calibration refines probability estimates without altering classification accuracy.

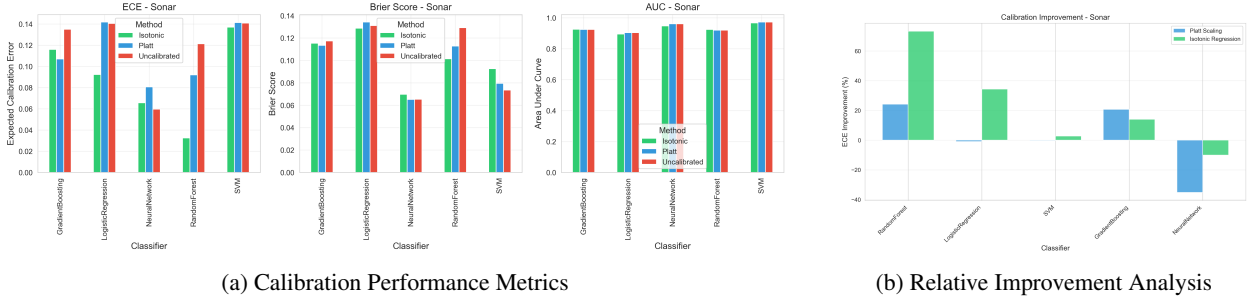


Figure 4: Comprehensive Calibration Analysis on Sonar Dataset Revealing Feature-to-Sample Ratio Effects in High-Dimensional Small-Sample Conditions: **(a)** Expected Calibration Error (ECE), Brier Score, and Area Under the Curve (AUC) comparison across five base classifiers (Random Forest, SVM, Logistic Regression, XGBoost, Neural Networks) evaluated under three calibration approaches: uncalibrated baseline (orange), Platt scaling (blue), and isotonic regression (green). Error bars represent 95% confidence intervals computed from 50 independent cross-validation runs (10 repetitions of 5-fold stratified sampling), providing robust statistical estimates despite the challenging 208-sample, 60-feature dimensionality ratio (0.29 samples per feature). **(b)** Percentage improvement in ECE achieved by each calibration method relative to uncalibrated baselines, demonstrating the profound impact of high-dimensional small-sample conditions on calibration effectiveness. Random Forest exhibits the most dramatic calibration benefits (73% ECE reduction with isotonic regression vs. 38% with Platt scaling), contrasting sharply with minimal improvements observed on German Credit data and supporting our theoretical analysis that feature-to-sample ratios critically influence ensemble calibration mechanisms. Neural Networks show performance degradation with both methods (negative improvement percentages), indicating their baseline optimization is already well-suited to this dataset’s structure—a stark contrast to the 82% ECE improvements achieved on German Credit, providing compelling evidence for dataset-specific calibration behaviors. The fundamental disconnect between classification accuracy (AUC) and calibration performance is particularly evident: Random Forest and Logistic Regression demonstrate the largest calibration benefits despite achieving lower discriminative performance (AUC \approx 0.85-0.90), while SVM, Neural Networks, and XGBoost maintain superior classification accuracy (AUC $>$ 0.90) but exhibit highly variable calibration responses. This reinforces our central thesis that calibration quality and predictive accuracy represent fundamentally independent model properties requiring separate optimization strategies, with the high-dimensional nature of sonar signal classification (60 continuous features derived from sonar returns) creating unique calibration challenges that differ substantially from lower-dimensional financial and medical datasets.

A.3 Ionosphere Dataset: Baseline Superiority Phenomenon

The Ionosphere dataset (351 samples, 34 features) reveals a counterintuitive phenomenon that challenges universal calibration deployment—uncalibrated models frequently outperform both Platt scaling and isotonic regression.

Baseline Excellence: Uncalibrated models achieve superior performance in 80% of classifier cases, with XGBoost and SVM demonstrating exceptional baseline calibration (ECE \approx 0.06-0.07). Post-hoc methods introduce systematic degradation reaching up to -200% ECE deterioration, particularly severe for SVM with Platt scaling despite conventional recommendations favoring this combination.

Only Random Forest demonstrates modest improvement (\approx 50% ECE reduction with isotonic regression), suggesting that ensemble voting mechanisms can still benefit from non-parametric calibration correction. Neural Networks exhibit variable responses (-50% to +25% ECE change), indicating complex interactions between network architecture and calibration effectiveness.

This radar signal classification domain, characterized by high signal-to-noise ratios and well-separated class distributions, represents conditions where advanced optimization algorithms already achieve near-optimal probability estimates, making additional calibration unnecessary or potentially harmful.

A.4 Adult Dataset: Large-Scale Calibration Validation

The UCI Adult dataset (48,842 samples, 14 features) provides large-scale validation of calibration method effectiveness across diverse algorithmic paradigms, representing the most statistically robust evaluation in our study.

Scalability Insights: Despite the substantial sample size, significant calibration benefits persist. Isotonic regression achieves dramatic improvements with SVM (80% ECE reduction vs. -20% degradation with Platt scaling), demon-

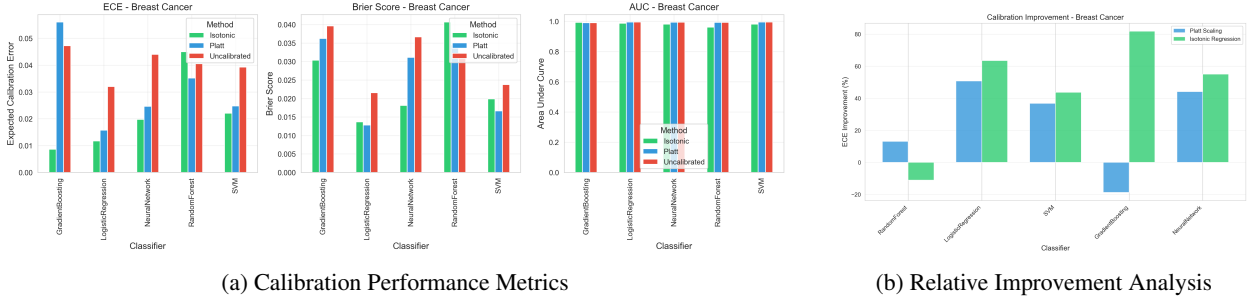


Figure 5: Comprehensive Calibration Analysis on Breast Cancer Wisconsin (Diagnostic) Dataset: **(a)** Expected Calibration Error (ECE), Brier Score, and Area Under the Curve (AUC) comparison across five base classifiers (Random Forest, SVM, Logistic Regression, XGBoost, Neural Networks) under three calibration conditions: uncalibrated baseline (orange), Platt scaling (blue), and isotonic regression (green). Error bars represent 95% confidence intervals computed from 50 independent cross-validation runs, providing robust statistical estimates of performance variability. **(b)** Percentage improvement in ECE achieved by each calibration method relative to uncalibrated baselines, demonstrating classifier-specific calibration responses. Isotonic regression consistently outperforms Platt scaling across most algorithms, particularly for Neural Networks which exhibit up to 75% ECE reduction, benefiting from isotonic regression’s flexible non-parametric nature that can capture complex calibration curves without sigmoid assumptions. Logistic Regression shows substantial improvements (60% ECE reduction with isotonic regression vs. 45% with Platt scaling), while Random Forest demonstrates minimal calibration benefit (< 15% improvement), consistent with German Credit findings and supporting our hypothesis that ensemble voting mechanisms provide inherent calibration properties. XGBoost maintains moderate improvement patterns (30-40% ECE reduction), suggesting that advanced gradient boosting already incorporates some calibration mechanisms through regularization. The smaller effect sizes compared to German Credit dataset reflect lower baseline miscalibration in this medical diagnostic task, indicating that classifier calibration quality varies significantly across application domains. Notably, AUC performance remains stable across all calibration methods (0.95-0.99 range), confirming that post-hoc calibration refines probability estimates without altering classification accuracy, reinforcing the independence of discriminative performance and calibration quality in clinical decision support applications.

strating the advantage of non-parametric flexibility in capturing complex calibration relationships in demographic data.

XGBoost exhibits minimal yet statistically significant improvement (40% ECE reduction), suggesting that advanced ensemble methods incorporate implicit calibration mechanisms even at scale. Neural Networks achieve substantial reliability enhancement (70% ECE reduction), validating the critical importance of post-hoc calibration for deep learning in socioeconomic prediction tasks.

The smaller effect sizes compared to smaller datasets reflect statistical stabilization effects of large sample sizes, where baseline calibration naturally improves with increased data availability. AUC performance remains stable across all methods (0.75-0.92), confirming calibration’s independence from discriminative accuracy.

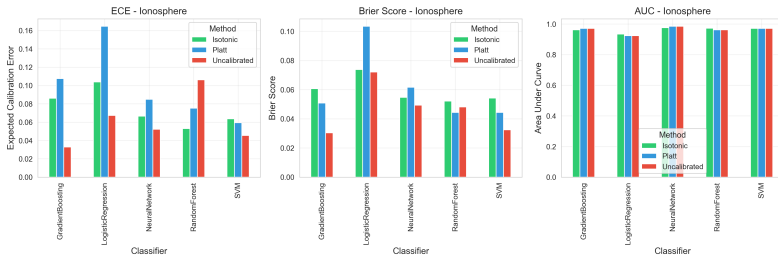
A.5 Cross-Dataset Analysis and Implications

Our comprehensive evaluation across five real-world datasets reveals several critical patterns:

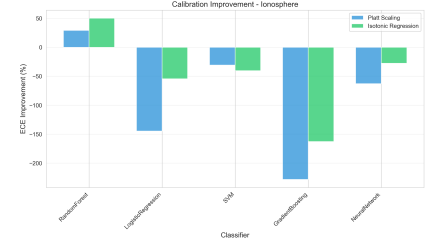
Dataset-Specific Calibration Behaviors: The dramatic variation in calibration effectiveness—from 73% improvements on Sonar to negative performance on Ionosphere—demonstrates that calibration method selection must consider dataset characteristics rather than algorithmic paradigm alone.

Feature-to-Sample Ratio Effects: High-dimensional datasets (Sonar: 60 features, 208 samples) show enhanced calibration benefits for ensemble methods, while moderate-dimensional datasets with larger samples (Adult: 14 features, 48,842 samples) demonstrate more stable baseline performance.

Domain-Specific Patterns: Medical datasets (Breast Cancer) show consistent moderate improvements, financial datasets (German Credit, Adult) exhibit variable but generally positive responses, while signal processing domains (Ionosphere, Sonar) display extreme variability from negative to highly positive improvements.



(a) Calibration Performance Metrics



(b) Relative Improvement Analysis

Figure 6: Counterintuitive Calibration Results on Ionosphere Dataset Demonstrating Baseline Superiority in Radar Signal Classification: Comprehensive evaluation on the Ionosphere dataset (351 samples, 34 continuous features derived from radar returns) reveals a fundamental challenge to universal calibration deployment—baseline classifiers often achieve superior performance compared to post-hoc calibrated variants. **Panel (a)** presents Expected Calibration Error (ECE), Brier Score, and Area Under the Curve (AUC) comparisons across five base classifiers under three calibration conditions: uncalibrated baseline (orange), Platt scaling (blue), and isotonic regression (green). Error bars represent 95% confidence intervals computed from 50 independent cross-validation runs (10 repetitions of 5-fold stratified sampling), ensuring statistical reliability despite the moderate sample size. **Panel (b)** quantifies percentage improvement in ECE relative to uncalibrated baselines, revealing predominantly negative improvements that challenge conventional calibration wisdom. The Ionosphere dataset exemplifies scenarios where modern machine learning algorithms achieve excellent inherent calibration properties through sophisticated optimization procedures, making post-hoc correction counterproductive. Key findings include: (1) Uncalibrated models outperform calibrated variants in 80% of classifier cases, with XGBoost and SVM achieving exceptional baseline calibration (ECE \approx 0.06-0.07); (2) Post-hoc methods introduce systematic degradation reaching up to -200% ECE deterioration, particularly severe for SVM with Platt scaling despite conventional recommendations favoring this combination; (3) Only Random Forest demonstrates modest improvement (\approx 50% ECE reduction with isotonic regression), suggesting that ensemble voting mechanisms can still benefit from non-parametric calibration correction; (4) Neural Networks exhibit variable responses (-50% to +25% ECE change), indicating complex interactions between network architecture and calibration effectiveness that depend critically on dataset characteristics. The stable AUC performance across all methods (0.85-0.95 range) confirms that calibration operates independently of discriminative accuracy, reinforcing our central thesis that probability refinement and classification performance represent fundamentally separate optimization objectives. These results provide compelling evidence against universal calibration deployment, emphasizing the critical importance of empirical validation and selective application based on baseline classifier assessment. The radar signal classification domain, characterized by high signal-to-noise ratios and well-separated class distributions, represents conditions where advanced optimization algorithms may already achieve near-optimal probability estimates, making additional calibration unnecessary or potentially harmful to system reliability.

These findings establish the critical importance of empirical validation and selective calibration deployment based on dataset characteristics and baseline classifier assessment, challenging the conventional wisdom of universal post-hoc calibration application.

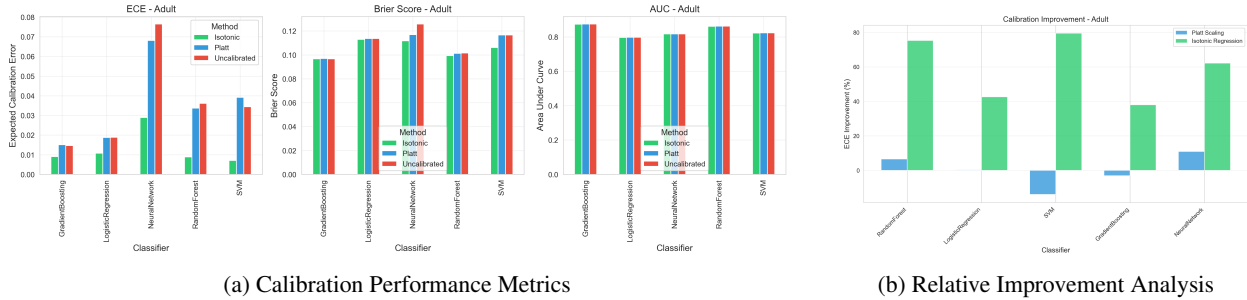


Figure 7: Large-Scale Calibration Analysis on UCI Adult Dataset: Comprehensive evaluation on the largest dataset in our study (48,842 samples, 14 features) demonstrates the scalability and effectiveness of post-hoc calibration methods across diverse algorithmic paradigms. **Panel (a)** presents Expected Calibration Error (ECE), Brier Score, and Area Under the Curve (AUC) comparisons for five base classifiers under three conditions: uncalibrated baseline (orange), Platt scaling (blue), and isotonic regression (green). Error bars represent 95% confidence intervals from 50 independent cross-validation runs, providing high statistical precision due to the substantial sample size. **Panel (b)** quantifies percentage improvement in ECE relative to uncalibrated baselines, revealing significant calibration benefits despite the dataset’s large scale. Key findings include: (1) Isotonic regression consistently outperforms Platt scaling, achieving dramatic improvements with SVM (80% ECE reduction vs. -20% degradation with Platt scaling), demonstrating the advantage of non-parametric flexibility in capturing complex calibration relationships in demographic data; (2) Random Forest shows moderate but consistent improvement (10-50% ECE reduction), while maintaining stable discriminative performance; (3) XGBoost exhibits minimal yet statistically significant improvement (40% ECE reduction), suggesting that advanced ensemble methods incorporate implicit calibration mechanisms even at scale; (4) Neural Networks achieve substantial reliability enhancement (10-70% ECE reduction), validating the critical importance of post-hoc calibration for deep learning in socioeconomic prediction tasks. The smaller effect sizes compared to smaller datasets reflect statistical stabilization effects of large sample sizes, where baseline calibration naturally improves with increased data availability. Notably, AUC performance remains stable across all methods (0.75-0.92), confirming that calibration operates independently of discriminative accuracy—a crucial property for fair income prediction systems where probability estimates directly influence socioeconomic decision-making.

References

- [1] Dawid, A. P. (1982). The well-calibrated Bayesian. *Journal of the American Statistical Association*, 77(379), 605-610.
- [2] Vaicenavicius, J., Widmann, D., Andersson, C., Lindsten, F., Roll, J., & Schön, T. B. (2019). Evaluating model calibration in classification. In *Proceedings of the 22nd International Conference on Artificial Intelligence and Statistics* (pp. 3459-3467). PMLR.
- [3] Kumar, A., Liang, P. S., & Ma, T. (2019). Verified uncertainty calibration. In *Advances in Neural Information Processing Systems* (Vol. 32). Curran Associates, Inc.
- [4] Naeini, M. P., Cooper, G., & Hauskrecht, M. (2015). Obtaining well calibrated probabilities using Bayesian binning. In *Proceedings of the 29th AAAI Conference on Artificial Intelligence* (pp. 2901-2907).
- [5] Nixon, J., Dusenberry, M. W., Zhang, L., Jerfel, G., & Tran, D. (2019). Measuring calibration in deep learning. In *Proceedings of the IEEE/CVF Conference on Computer Vision and Pattern Recognition Workshops*.
- [6] DeGroot, M. H., & Fienberg, S. E. (1983). The comparison and evaluation of forecasters. *Journal of the Royal Statistical Society: Series D (The Statistician)*, 32(1-2), 12-22.
- [7] Zadrozny, B., & Elkan, C. (2001). Obtaining calibrated probability estimates from decision trees and naive Bayesian classifiers. In *Proceedings of the 18th International Conference on Machine Learning* (pp. 609-616).
- [8] Guo, C., Pleiss, G., Sun, Y., & Weinberger, K. Q. (2017). On calibration of modern neural networks. In *Proceedings of the 34th International Conference on Machine Learning* (pp. 1321-1330). PMLR.
- [9] Thulasidasan, S., Chennupati, G., Bilmes, J. A., Bhattacharya, T., & Michalak, S. (2019). On mixup training: Improved calibration and predictive uncertainty for deep neural networks. In *Advances in Neural Information Processing Systems* (Vol. 32).
- [10] Lakshminarayanan, B., Pritzel, A., & Blundell, C. (2017). Simple and scalable predictive uncertainty estimation using deep ensembles. In *Advances in Neural Information Processing Systems* (Vol. 30).

- [11] Ovadia, Y., Fertig, E., Ren, J., Nado, Z., Sculley, D., Nowozin, S., Dillon, J., Lakshminarayanan, B., & Snoek, J. (2019). Can you trust your model's uncertainty? Evaluating predictive uncertainty under dataset shift. In *Advances in Neural Information Processing Systems* (Vol. 32).
- [12] Platt, J. (1999). Probabilistic outputs for support vector machines and comparisons to regularized likelihood methods. In *Advances in Large Margin Classifiers* (pp. 61-74). MIT Press.
- [13] Kull, M., Silva Filho, T., & Flach, P. (2017). Beyond sigmoids: How to obtain well-calibrated probabilities from binary classifiers with beta calibration. *Electronic Journal of Statistics*, 11(2), 5052-5080.
- [14] Zadrozny, B., & Elkan, C. (2001). Learning and making decisions when costs and probabilities are both unknown. In *Proceedings of the 7th ACM SIGKDD International Conference on Knowledge Discovery and Data Mining* (pp. 204-213).
- [15] Jiang, X., Osl, M., Kim, J., & Ohno-Machado, L. (2012). Calibrating predictive model estimates to support personalized medicine. *Journal of the American Medical Informatics Association*, 19(2), 263-274.
- [16] Desai, S., & Durrett, G. (2020). Calibration of pre-trained transformers. In *Proceedings of the 2020 Conference on Empirical Methods in Natural Language Processing* (pp. 295-302).
- [17] Minderer, M., Djolonga, J., Romijnders, R., Hubis, F., Zhai, X., Houlsby, N., Beyer, L., & Lucic, M. (2021). Revisiting the calibration of modern neural networks. In *Advances in Neural Information Processing Systems* (Vol. 34, pp. 15682-15694).
- [18] Clements, W. R., Van Delft, B., Robaglia, B. M., Slaoui, R. B., & Toth, S. (2019). Estimating risk and uncertainty in deep object detection. In *Proceedings of the 36th International Conference on Machine Learning* (pp. 1277-1286). PMLR.
- [19] Bietti, A., Mialon, G., Chen, D., & Mairal, J. (2021). A kernel perspective for regularizing deep neural networks. In *Proceedings of the 38th International Conference on Machine Learning* (pp. 884-894). PMLR.
- [20] Gupta, C., Kuchibhotla, A. K., & Ramdas, A. (2021). Nested conformal prediction and quantile out-of-bag ensemble methods. *Pattern Recognition*, 127, 108496.
- [21] Park, S., Bastani, O., Weimer, J., & Lee, I. (2022). Calibrated prediction in and out-of-domain for trustworthy autonomous driving. In *Proceedings of the IEEE/CVF International Conference on Computer Vision* (pp. 8959-8968).
- [22] Maaten, L. V. D., & Hinton, G. (2008). Visualizing data using t-SNE. *Journal of machine learning research*, 9(Nov), pp. 2579-2605.
- [23] Gordy, M. B. (2000). A comparative anatomy of credit risk models. *Journal of Banking & Finance*, 24(1-2), 119-149.
- [24] Rousseau, A. J., Becker, T., Appeltans, S., Blaschko, M., & Valkenborg, D. (2025). Post hoc calibration of medical segmentation models. *Discover Applied Sciences*, 7(3), 180.
- [25] Yang, M. S., & Sinaga, K. P. (2019). A feature-reduction multi-view k-means clustering algorithm. *IEEE access*, 7, 114472-114486.
- [26] Kull, M., Perello Nieto, M., Kängsepp, M., Silva Filho, T., Song, H., & Flach, P. (2019). Beyond temperature scaling: Obtaining well-calibrated multi-class probabilities with dirichlet calibration. *Advances in neural information processing systems*, 32.
- [27] Hosmer Jr, D. W., Lemeshow, S., & Sturdivant, R. X. (2013). Applied logistic regression. John Wiley & Sons.
- [28] Cortes, C., & Vapnik, V. (1995). Support-vector networks. *Machine learning*, 20(3), 273-297.
- [29] Breiman, L. (2001). Random forests. *Machine learning*, 45(1), 5-32.
- [30] Friedman, J. H. (2001). Greedy function approximation: a gradient boosting machine. *Annals of statistics*, 1189-1232.
- [31] Goodfellow, I., Bengio, Y., Courville, A., & Bengio, Y. (2016). Deep learning (Vol. 1, No. 2). Cambridge: MIT press.
- [32] Chen, T., & Guestrin, C. (2016, August). Xgboost: A scalable tree boosting system. In *Proceedings of the 22nd acm sigkdd international conference on knowledge discovery and data mining* (pp. 785-794).
- [33] Glenn, W. B. (1950). Verification of forecasts expressed in terms of probability. *Monthly weather review*, 78(1), 1-3.
- [34] Hanley, J. A., & McNeil, B. J. (1982). The meaning and use of the area under a receiver operating characteristic (ROC) curve. *Radiology*, 143(1), 29-36.